

# What are the Proper Transport Models at the Nanoscale?



Semiclassical Transport Approaches  
Quantum Transport  
Atomistic Simulations

## Computational Electronics



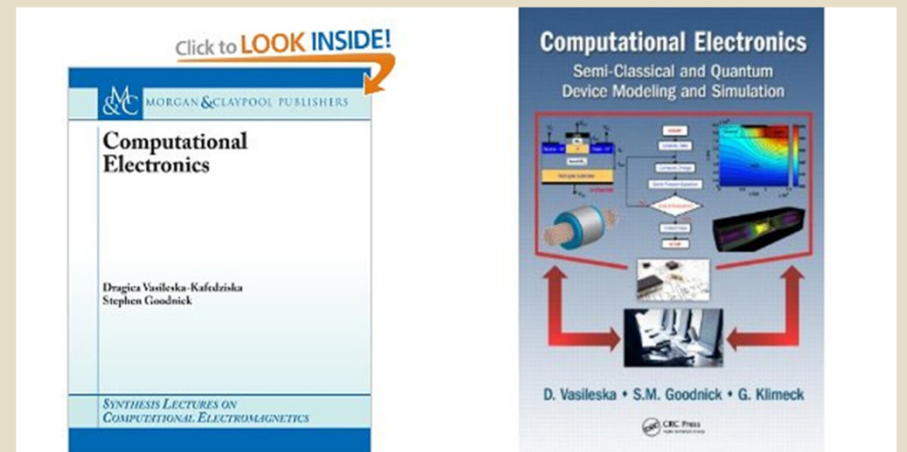
UNIVAC

ENIAC



Grace Hopper – first woman programmer

COMPUTEL



# Advantages and disadvantages of models



## Range of Validity of Different Methods

	$L \ll l_{e-ph}$			$L \sim l_{e-ph}$	$L \gg l_{e-ph}$
	$L < \lambda$	$L < l_{e-e}$	$L \gg l_{e-e}$		
<b>Transport Regime</b>	Quantum	Ballistic	Fluid	Fluid	Diffusive
<b>Scattering</b>	Rare	Rare	e-e (Many), e-ph (Few)		Many
<b>Model:</b>					
Drift-Diffusion					
Hydrodynamic		Quantum Hydrodynamic			
Monte Carlo					
Schrodinger/Green's Functions	Wave				
<b>Applications</b>	Nanowires, Superlattices	Ballistic Transistor	Current IC's	Current IC's	Older IC's

# What are the Proper Transport Models at the Nanoscale?



## Semiclassical Transport Approaches

Quantum Transport  
Atomistic Simulations

### Computational Electronics



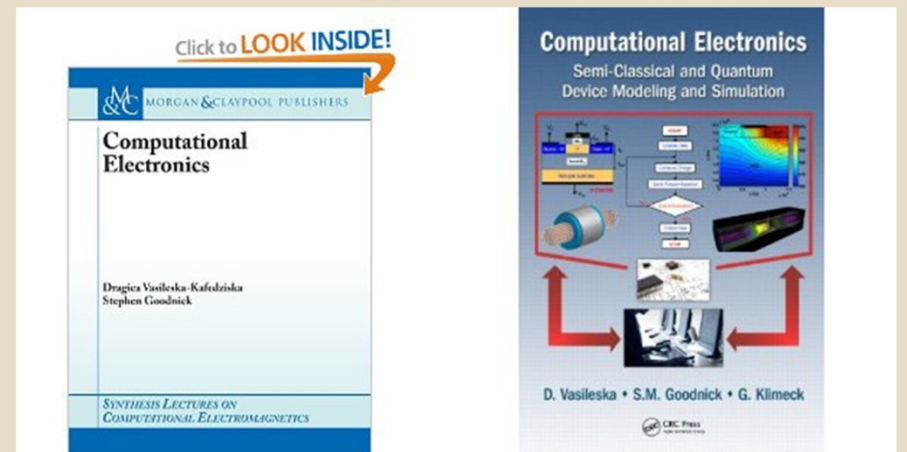
UNIVAC

ENIAC



Grace Hopper – first woman programmer

COMPUTEL



# Boltzmann Transport Equation



- In its most general form, the BTE equals to:

$$\begin{aligned} \frac{\partial f}{\partial t} + \vec{v} \cdot \nabla_r f + (-e)\vec{\mathcal{E}} \cdot \nabla_p f &= \frac{\partial f}{\partial t} \Big|_{coll} = \\ &= \sum_{i=1}^N \sum_{\vec{p}'} [S_i(\vec{p}', \vec{p}) f(\vec{r}, \vec{p}', t) - S_i(\vec{p}, \vec{p}') f(\vec{r}, \vec{p}, t)] \end{aligned}$$

- The collision integral on the RHS can be expressed as:

$$RHS = \sum_{\vec{p}'} \sum_{i=1}^N [S_i(\vec{p}', \vec{p}) f(\vec{r}, \vec{p}', t)] - f(\vec{r}, \vec{p}, t) \sum_{\vec{p}'} \sum_{i=1}^N S_i(\vec{p}, \vec{p}')$$

# Path Integral Solution of the BTE



- The path integral solution of the Boltzmann Transport Equation (BTE), where  $L=N\Delta t$  and  $t_n=n\Delta t$ , is of the form:

$$f_N(t) = \Delta t \sum_{m=0}^{N-1} \underbrace{f_m(p') S_{eff}(p', p + eE(N-m)\Delta t)}_{g_m(p + eE(N-m)\Delta t)} e^{-\Gamma(N-m)\Delta t}$$

K. K. Thornber and Richard P. Feynman, Phys. Rev. B 1, 4099 (1970).

# Path Integral Solution of the BTE



- The two-step procedure is then found by using  $N=1$ , which means that  $t=\Delta t$ , i.e.:

$$f_1(t) = \Delta t \sum_{p'} f_0(p') S_{eff}(p', p + eE\Delta t) e^{-\Gamma\Delta t}$$

$$g_0(p + eE\Delta t)$$

Intermediate function that describes the occupancy of the state  $(p+eE\Delta t)$  at time  $t=0$ , which can be changed due to scattering events **SCATTER**

Integration over a trajectory, i.e. probability that no scattering occurred within time integral  $\Delta t$

+

**FREE FLIGHT**

# Path Integral Solution of the BTE



- Using path integral formulation to the BTE we have shown that one can decompose the solution procedure into two components:

- **Carrier free-flights** that are interrupted by scattering events

$$\mathbf{k}(t) = \mathbf{k}(0) - \mathbf{e}(\mathbf{v} \times \mathbf{B} + \mathbf{E})t / \hbar$$

- **Memory-less scattering events** that change the momentum and the energy of the particle instantaneously

# Ways of solving the BTE

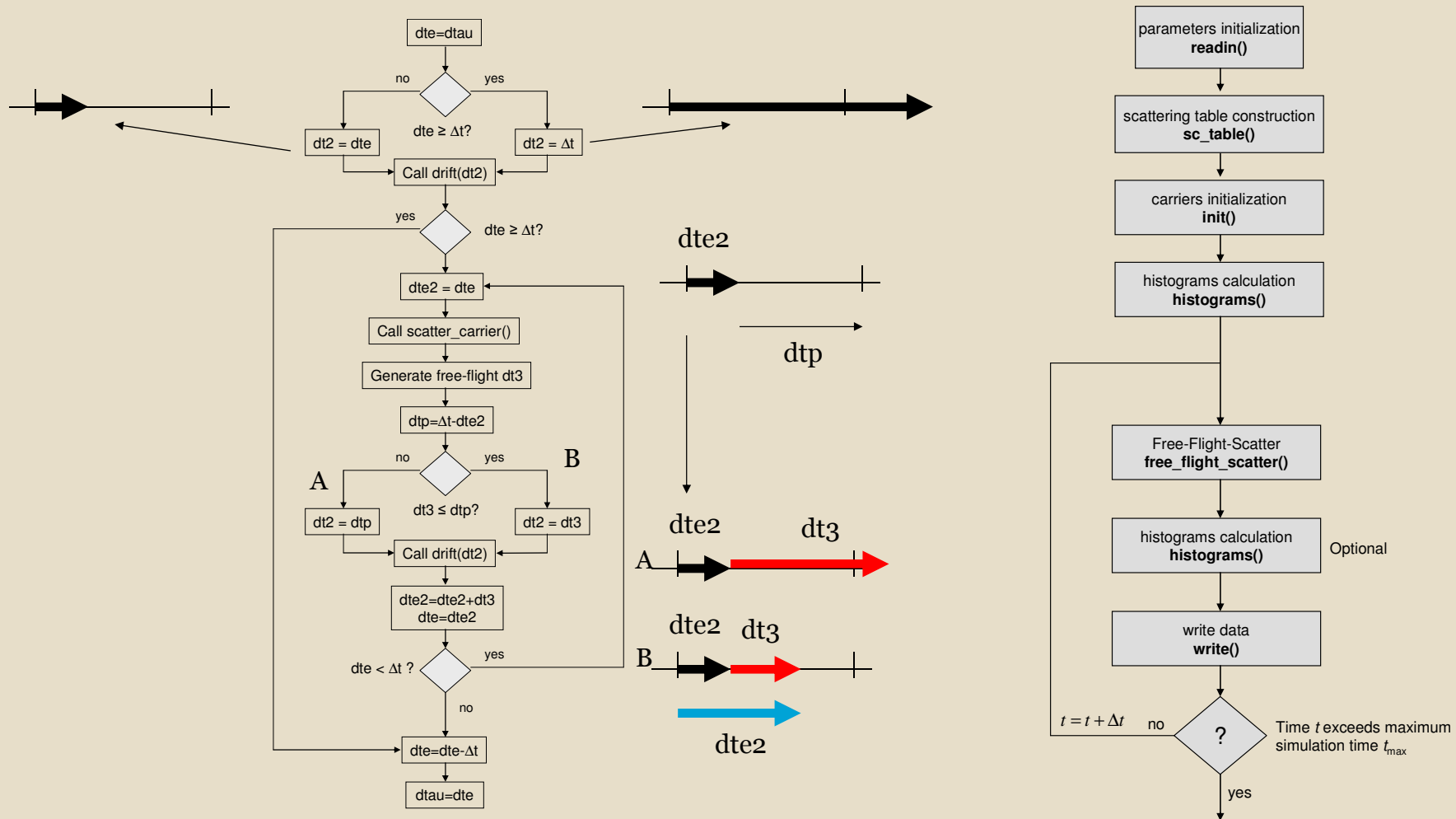


- **Single particle Monte Carlo Technique**
  - Follow single particle for long enough time to collect sufficient statistics
  - Practical for characterization of bulk materials or inversion layers
- **Ensemble Monte Carlo Technique**
  - **MUST BE USED** when modeling SEMICONDUCTOR DEVICES to have the complete self-consistency built in

Carlo Jacoboni and Lino Reggiani, The Monte Carlo method for the solution of charge transport in semiconductors with applications to covalent materials, Rev. Mod. Phys. 55, 645 - 705 (1983).



# Bulk MC Flow-Chart



# ASU's Particle-Based Device Simulator (Vasileska Group)



Initialize Material Parameters  
and Device Structure

Initialization includes Random Dopant Distribution and  
Unintentional Trap Specification



Monte Carlo Kernel:  
free-flight-scatter

Perform  
Particle-Mesh  
Coupling

Solve Poisson Equation

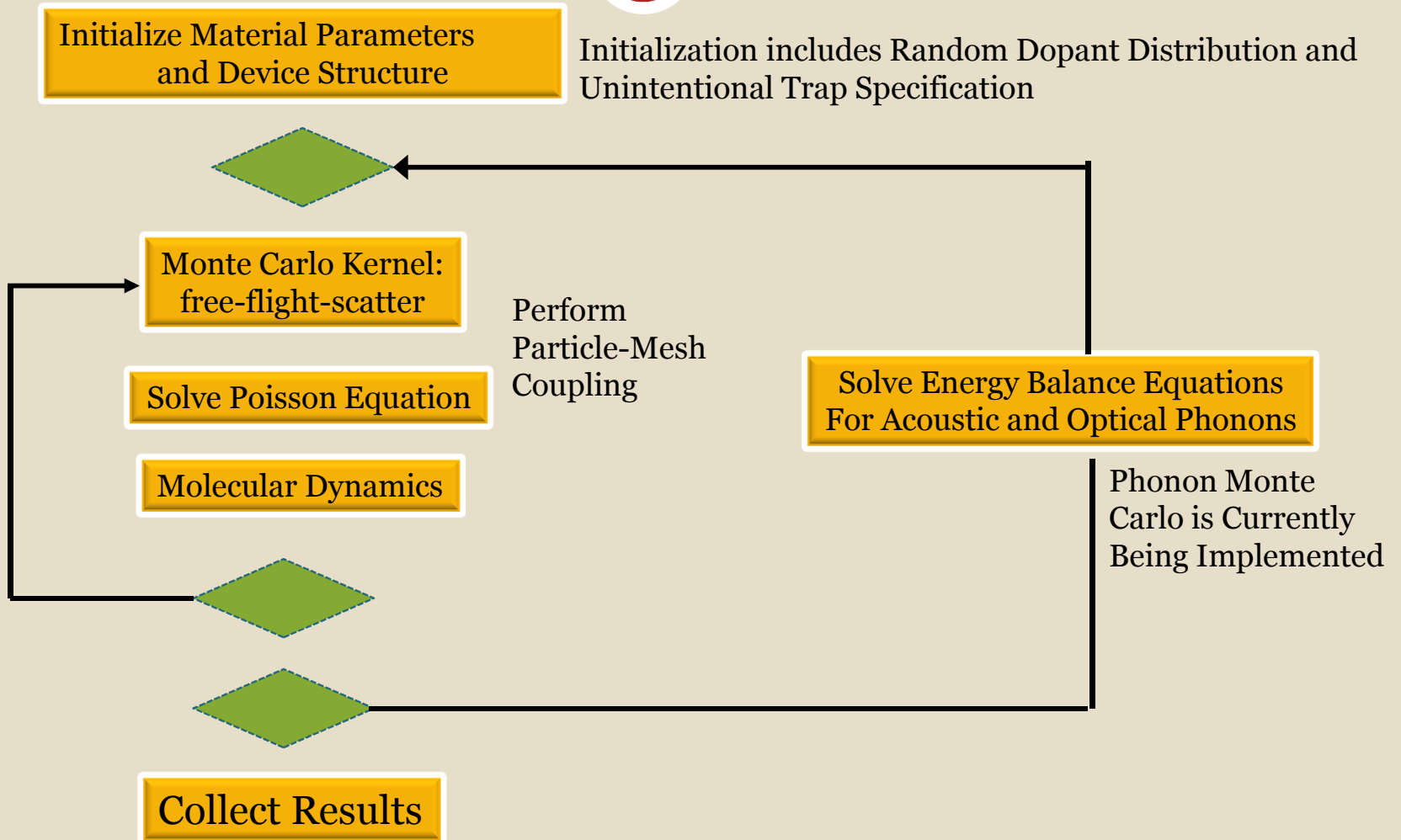
Solve Energy Balance Equations  
For Acoustic and Optical Phonons

Molecular Dynamics

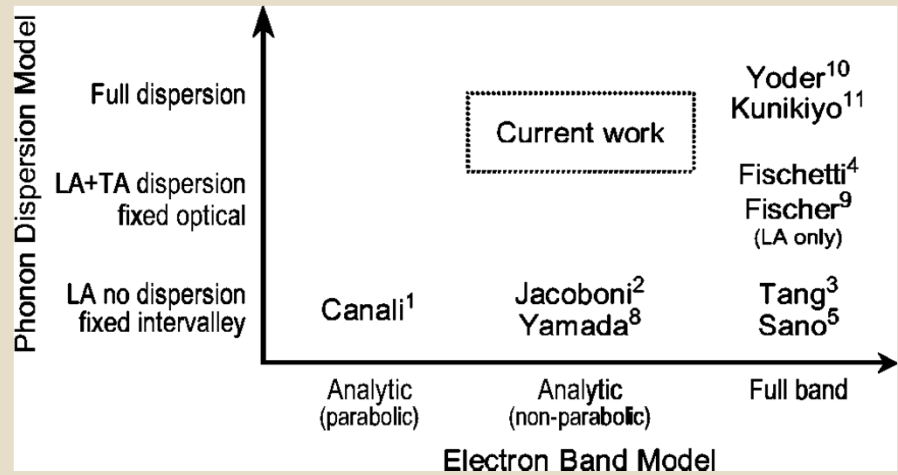
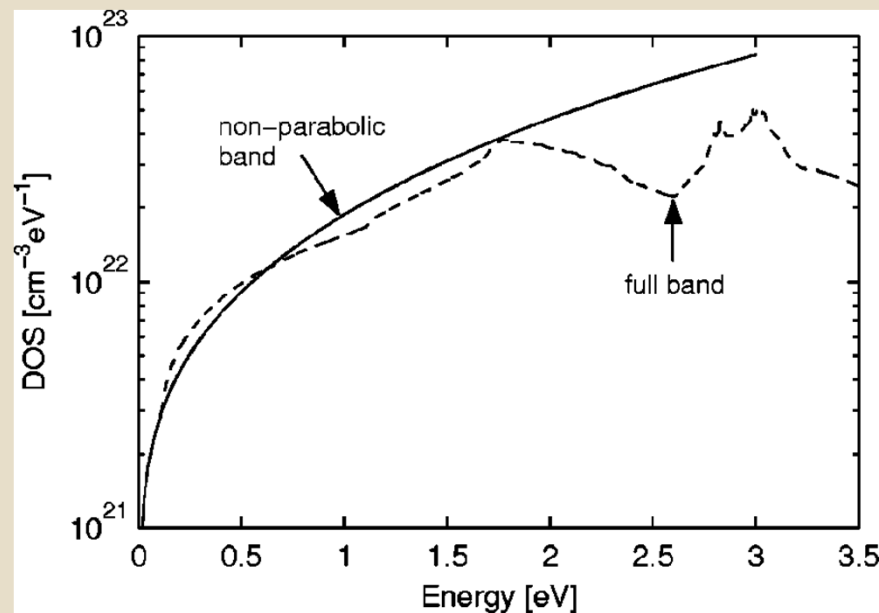
Phonon Monte  
Carlo is Currently  
Being Implemented



Collect Results



# The Monte Carlo Method - Non-parabolicity and Full-Band -



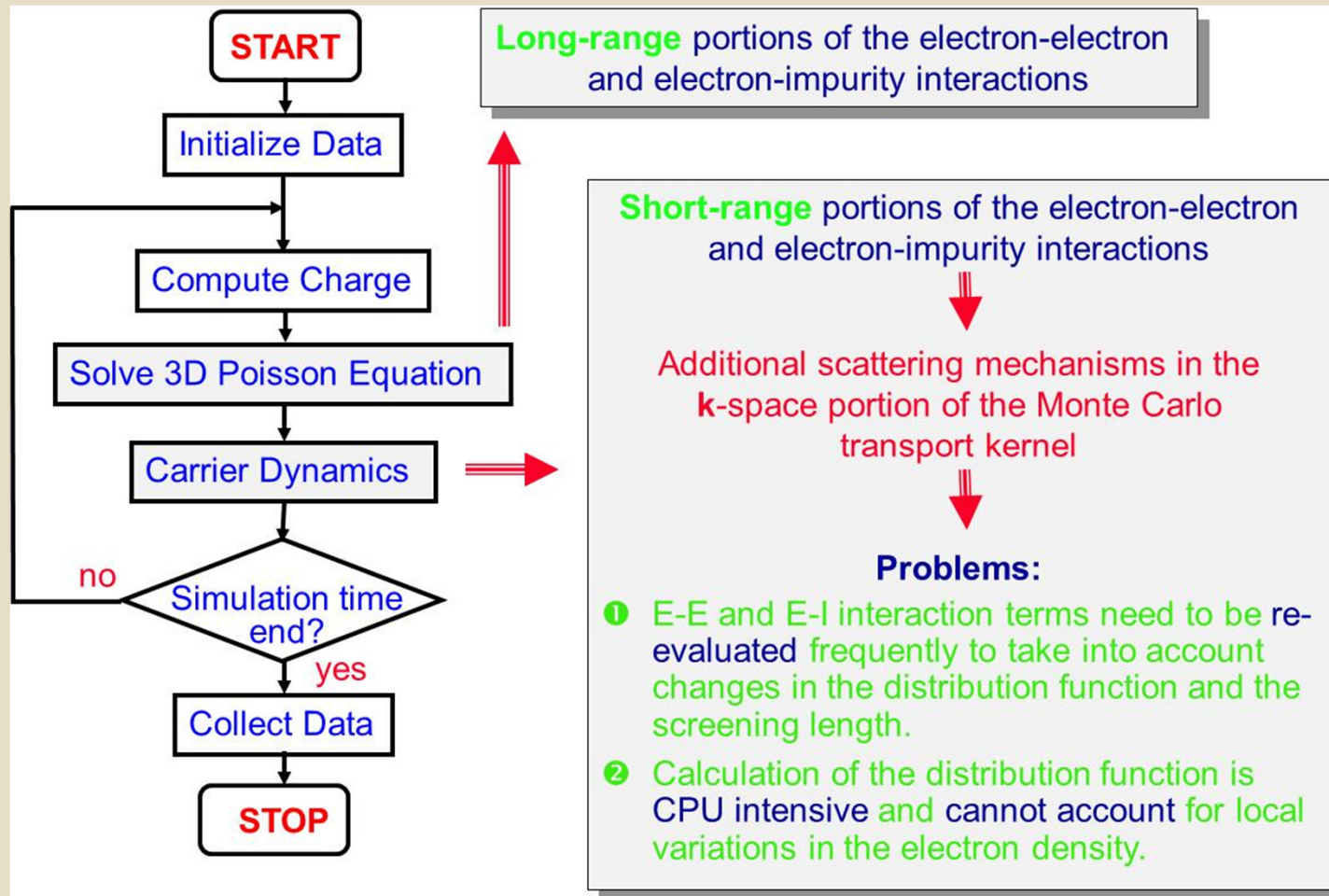
E. Pop, R. W. Dutton and K. E. Goodson, JOURNAL OF APPLIED PHYSICS VOLUME 96, NUMBER 9 1 NOVEMBER 2004

# Particle Based Device Simulators



**INCORPORATION OF THE SHORT-RANGE  
COULOMB INTERACTION**

# K-Space Approach



# Real-Space Approach



- Requires 3D device simulator, otherwise the method fails
- There are several variants of this method
  - Corrected Coulomb approach developed by Vasileska and Gross
  - Particle-particle-particle-mesh (p3m) method by Hockney and Eastwood
  - Fast Multipole method
- Corrected Coulomb approach and p3m method are almost equivalent in philosophy, FMM is very different
- Treatment of the short-range Coulomb interactions using any of these three methods accounts for:
  - Binary collisions + plasma (collective) excitations
  - Screening of the Coulomb interactions
  - Scattering from multiple impurities at the same time which is very important at high substrate doping densities

# Simulation Methodologies

## Method Complexity

P <sup>3</sup> M	FMM
$O(N+M\log M)$	$O(N)$

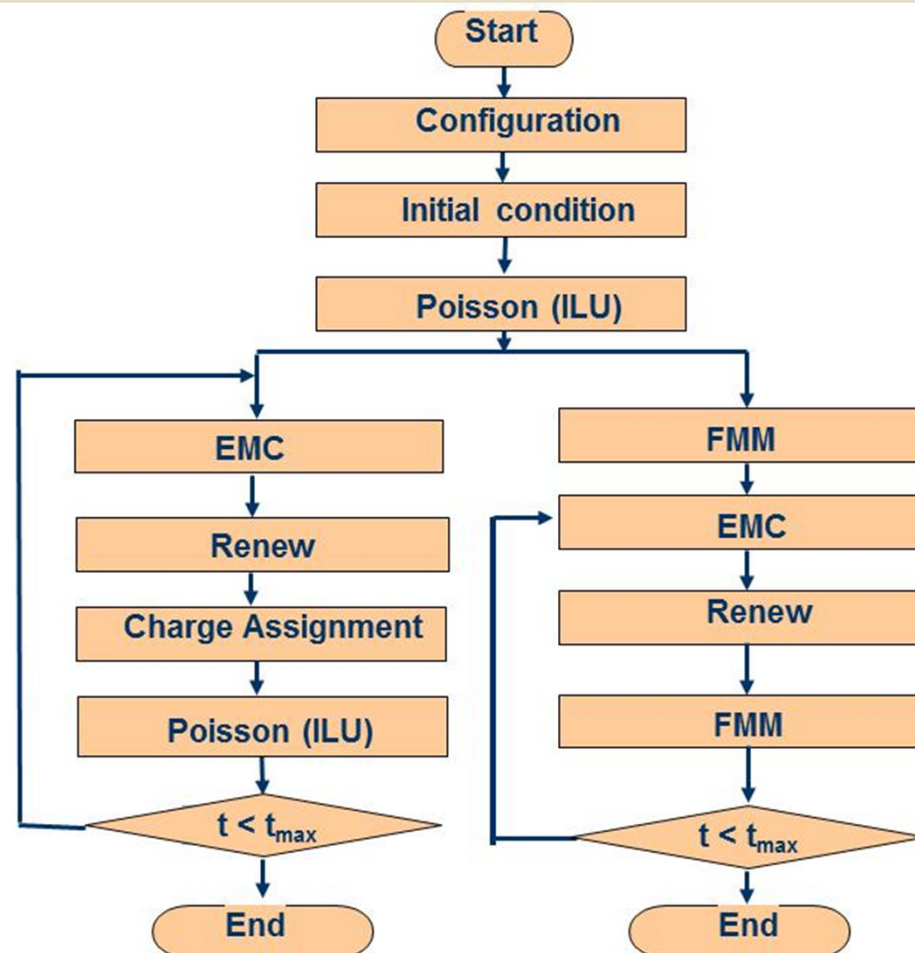
N=Number of particles

M=Number of Mesh Points

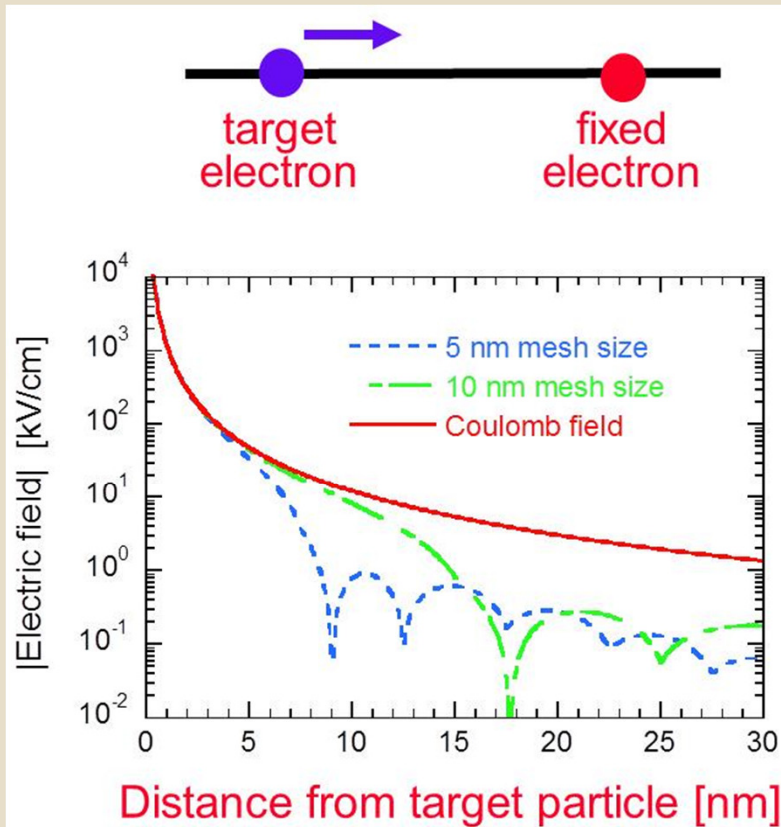
## Computation time

Machine: P-4 , 2GHz  
 Mesh points: 64X24X24  
 Particles: 690

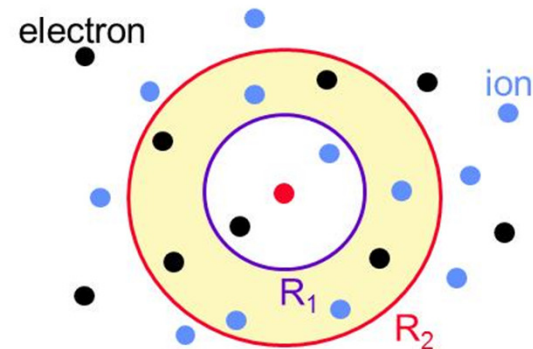
Time for each iteration	
P <sup>3</sup> M	FMM
~24 sec	<1sec



# Corrected Coulomb Approach



- ⊙ **Double-counting** of the Coulomb force is **eliminated**
- ⊙ **Limitation:** must use **uniform** mesh spacing
- ⊙ The generated look-up table gives us information about the **proper cut-off range**



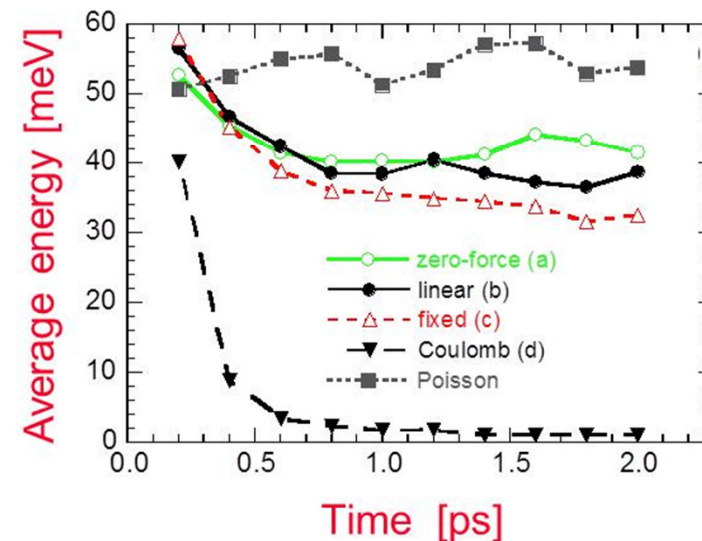
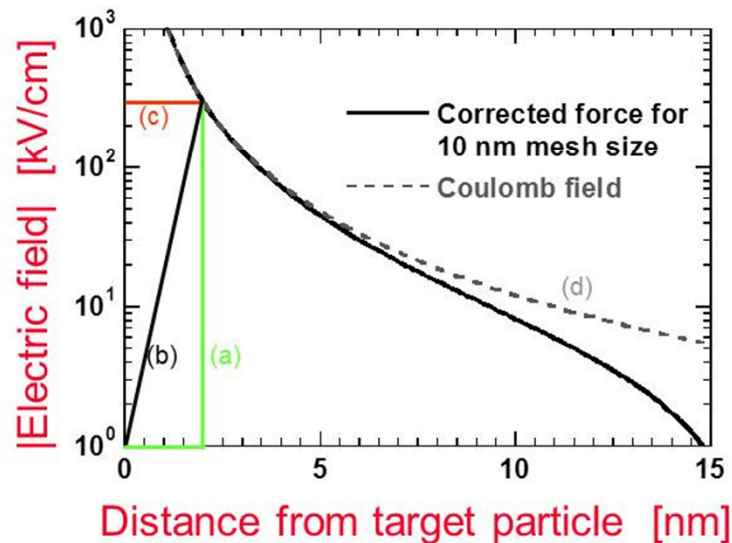
$R_2$  must be greater than  $2\times$  the mesh spacing



# Corrected Coulomb Approach – Cont'd



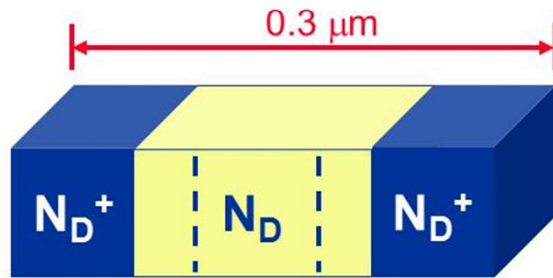
- ⦿ The use of the simple Coulomb interaction in the source and drain regions leads to electron trapping which, in turn, prevents the filling of the channel with electrons.
- ⦿ The carrier trapping can be eliminated through the use of modified short-range Coulomb correction force.



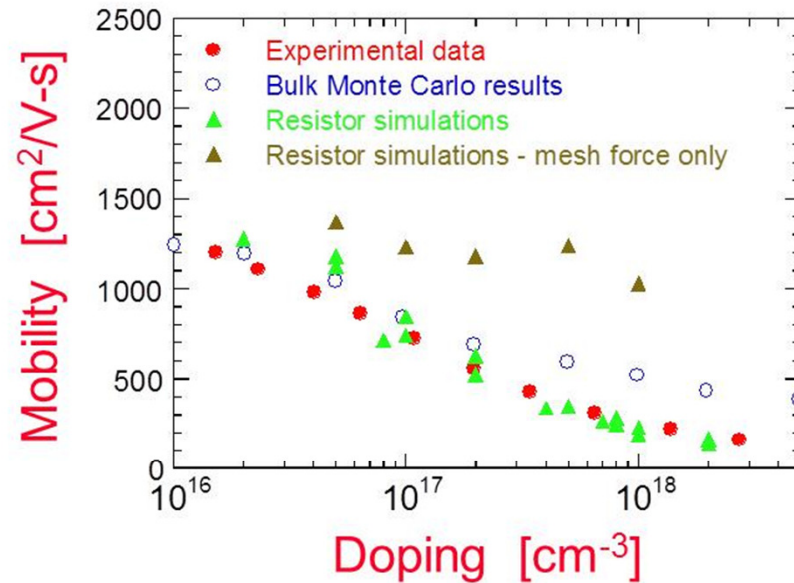
# Corrected Coulomb Approach – Cont'd



- ⊙ Doping of the  $N^+$ - regions:  
 $N_{D^+} = 10^{19} \text{ cm}^{-3}$ .
- ⊙ Mesh: uniform mesh spacing in all directions equal to 10 nm.
- ⊙ Cases considered:
  - Mesh force only
  - Mesh force + short-range  $e-e$  and  $e-i$  interaction terms

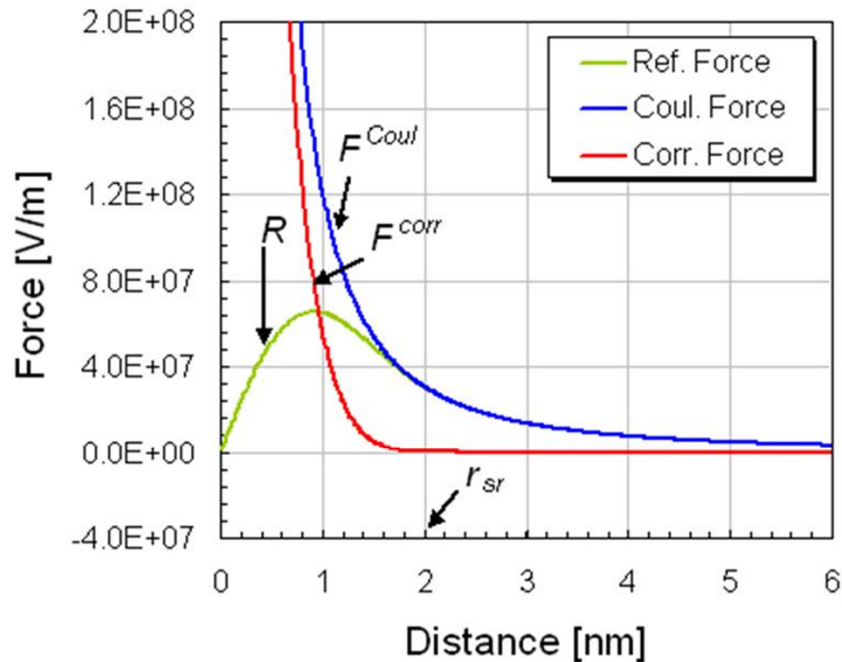


Low-field mobility:  $\mu = \frac{\bar{v}_{drift}}{E}$



- ⊙ The **mesh force only** does not give the correct doping dependence of the low-field electron mobility.
- ⊙ The inclusion of the **short-range interaction terms** gives simulation low-field mobility data in agreement with experimental values.

# P3M Approach



$$F_{ij}^{corr} = F_{ij}^{Coul} - R_{ij}$$

R. W. Hockney and J. W. Eastwood, *Computer Simulation Using Particles* (New York, McGraw-Hill, 1981).

Reference force replaces the mesh force and needed to avoid double counting of the short-range force.

The reference force should be equal to the mesh force inside the SR domain and equal to the Coulomb force outside the SR domain.

# P3M Approach – Cont'd



Smoothing of the total interparticle force between the long-and short-range domains can be thought of as ascribing a finite size to particle  $i$ .

A **sphere with uniformly decreasing density profile,  $S(r)$**  is a good choice for smoothing in three dimensions.

↓

$$S(r) = \begin{cases} \frac{48}{\pi r_{sr}^4} \left( \frac{r_{sr}}{2} - r \right), & r \leq r_{sr} / 2 \\ 0, & \text{otherwise,} \end{cases}$$

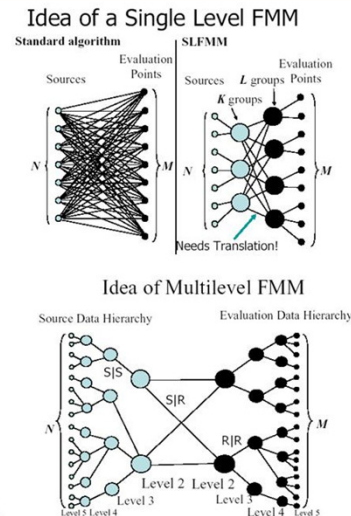
$$\left\{ \begin{array}{ll} R_{ij}(r) = \frac{q_i q_j}{4\pi\epsilon} \times \frac{1}{35r_{sr}^2} (224\xi - 224\xi^3 + 70\xi^4 + 48\xi^5 - 21\xi^6) & \xi = \frac{2r}{r_{sr}} \text{ and } 0 \leq r \leq r_{sr} / 2 \\ R_{ij}(r) = \frac{q_i q_j}{4\pi\epsilon} \times \frac{1}{35r_{sr}^2} \left( \frac{12}{\xi^2} - 224 + 896\xi - 840\xi^2 + 224\xi^3 + 70\xi^4 - 48\xi^5 + 7\xi^6 \right) & r_{sr} / 2 \leq r \leq r_{sr} \\ R_{ij}(r) = \frac{q_i q_j}{4\pi\epsilon} \times \frac{1}{r^2} & r > r_{sr} \end{array} \right.$$

# FMM Approach

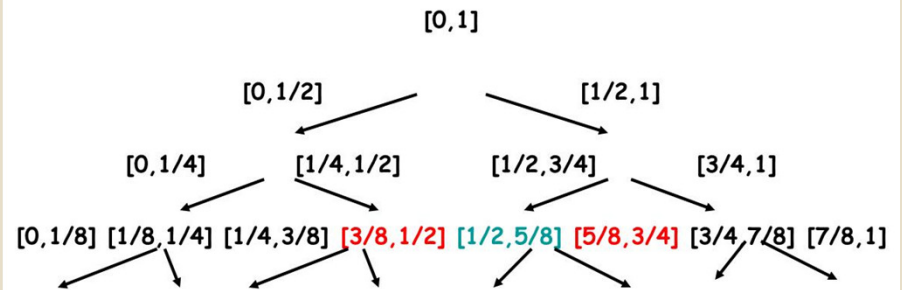


- Introduced by Rokhlin & Greengard in 1987.
- Called one of the 10 most significant advances in computing of the 20<sup>th</sup> century.
- For a given precision  $\varepsilon$ , the FMM achieves the evaluation in  $O(M+N)$  operations.
- Edelman: "FMM is all about adding functions".

V. Rokhlin and L. Greengard, *J. Comp. Phys.*, Vol. 73, pp. 325-348, 1987.



- Consider the following binary tree structure induced by a uniform subdivision of the unit interval:



- To approximately evaluate  $s(x)$  in the panel  $[1/2,5/8]$ , we have:

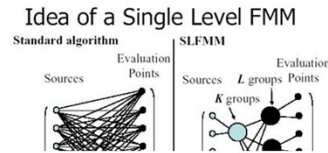
$$s(x) \approx s_{[3/8,1/2]}(x) + s_{[1/2,5/8]}(x) + s_{[5/8,3/4]}(x) + r_{[1/4,3/8]}(x) + r_{[3/4,7/8]}(x) + r_{[7/8,1]}(x) + r_{[0,1/4]}(x)$$

L. Greengard and V. Rokhlin. On the Efficient Implementation of the Fast Multipole Algorithm. Department of Computer Science Research Report 602, Yale University (1988).

# FMM Approach



- Introduced by Rokhlin & Greengard in 1987.
- Called one of the 10 most significant advances in

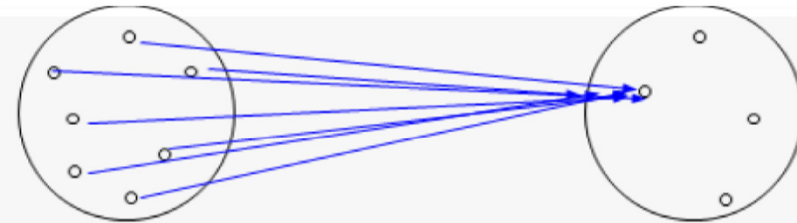


- Consider the following binary tree structure induced by a uniform subdivision of the unit interval:

[0,1]

$$\begin{aligned}
 \Phi(\mathbf{x}) &= \sum_{i=1}^N \frac{q_i}{|\mathbf{x} - \mathbf{y}_i|} \\
 &= \sum_{i=1}^N q_i \sum_{k=1}^p \psi_k(\mathbf{y}_i) \phi_k(\mathbf{x}) \\
 &= \sum_{k=1}^p \phi_k(\mathbf{x}) \sum_{i=1}^N q_i \psi_k(\mathbf{y}_i) \\
 &= \sum_{k=1}^p \phi_k(\mathbf{x}) A_k
 \end{aligned}$$

L. Greengard and V. Rokhlin, "A Fast Algorithm for Particle Simulations", J. Comp. Phys. V. 135, 280-292 (1997).

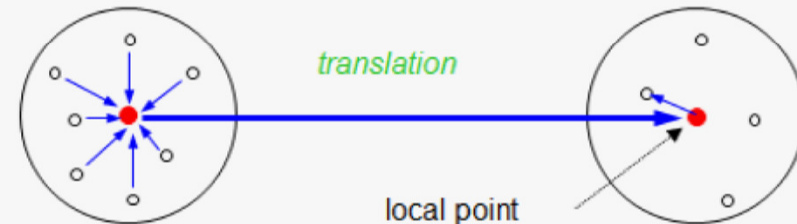


distant particles

local particles

*multipole moment*

*local expansion*



*translation*

local point

distant particles

local particles

# FMM Approach



- Introduced by Greengard in
- Called one of the significant

1. A detailed/comprehensive discussion may be found in:  
L. Greengard and V. Rokhlin, "A Fast Algorithm for Particle Simulations",  
Jour. Comp. Physics, Vol. 135, pp. 280-292, 1997.

2. Here we present a first-order correction method for the channel charges with the method of images:

*For a point charge  $q$  lying in a dielectric  $\epsilon_1$  distance  $x = d$  from the plane boundary between  $\epsilon_1$  and a second dielectric  $\epsilon_2$ , the given charge plus an image charge  $q(\epsilon_1 - \epsilon_2)/(\epsilon_1 + \epsilon_2)$  placed at  $x = -d$  with all space filled by a dielectric  $\epsilon_1$  may be used to compute the potential for any point  $x > 0$ .*

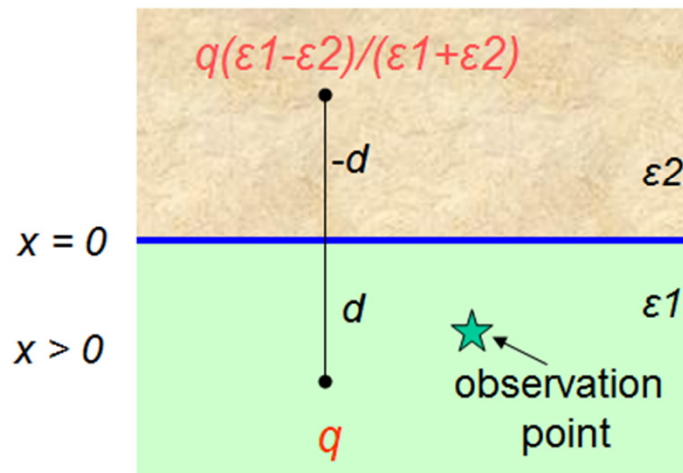
$$\Phi(x) =$$

=

=

=

L. Greengard  
Simulations

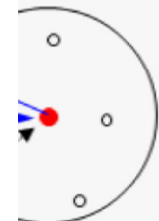


induced by a



articles

expansion

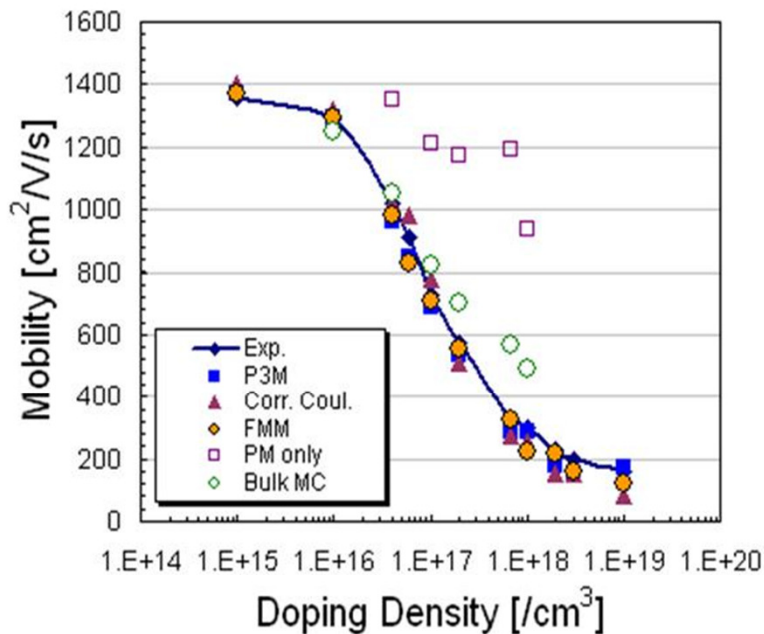


articles

# Resistor Simulations



## Resistor Simulation:



Method	Time/iteration
P <sup>3</sup> M	39 sec
FMM	17 sec

No. of monopole charges: ~22000  
Mesh: 40 x 25 x 25

- Uniform mesh (40 x 25 x 25)
- An external field of 1kV/cm was applied to ensure linear region of operation.
- The drift velocity was averaged over 5ps with an interval time of 0.1 ps. The first 1.5 ps data were discarded.



# Particle-Based Device Simulators



**INCORPORATION OF SELF-HEATING EFFECTS**

# ASU (Vasileska) Model for Self-Heating Effects



$$\left( \frac{\partial}{\partial t} + v_e(\mathbf{k}) \cdot \nabla_r + \frac{e}{\hbar} E(\mathbf{r}) \cdot \nabla_k \right) f = \sum_q \left\{ W_{e,q}^{k+q \rightarrow k} + W_{a,-q}^{k+q \rightarrow k} - W_{e,-q}^{k \rightarrow k+q} - W_{a,q}^{k \rightarrow k+q} \right\}$$

$$\left( \frac{\partial}{\partial t} + v_p(q) \cdot \nabla_r \right) g = \sum_k \left\{ W_{e,q}^{k+q \rightarrow k} - W_{a,q}^{k \rightarrow k+q} \right\} + \left( \frac{\partial g}{\partial t} \right)_{p-p}$$



J. Lai and A. Majumdar, "Concurrent thermal and electrical modeling of submicrometer silicon devices", J. Appl. Phys. , Vol. 79, 7353 (1996).

$$C_{LO} \frac{\partial T_{LO}}{\partial t} = \frac{3nk_B}{2} \left( \frac{T_e - T_L}{\tau_{e-LO}} \right) + \frac{nm^* v_d^2}{2\tau_{e-LO}} - C_{LO} \left( \frac{T_{LO} - T_A}{\tau_{LO-A}} \right),$$

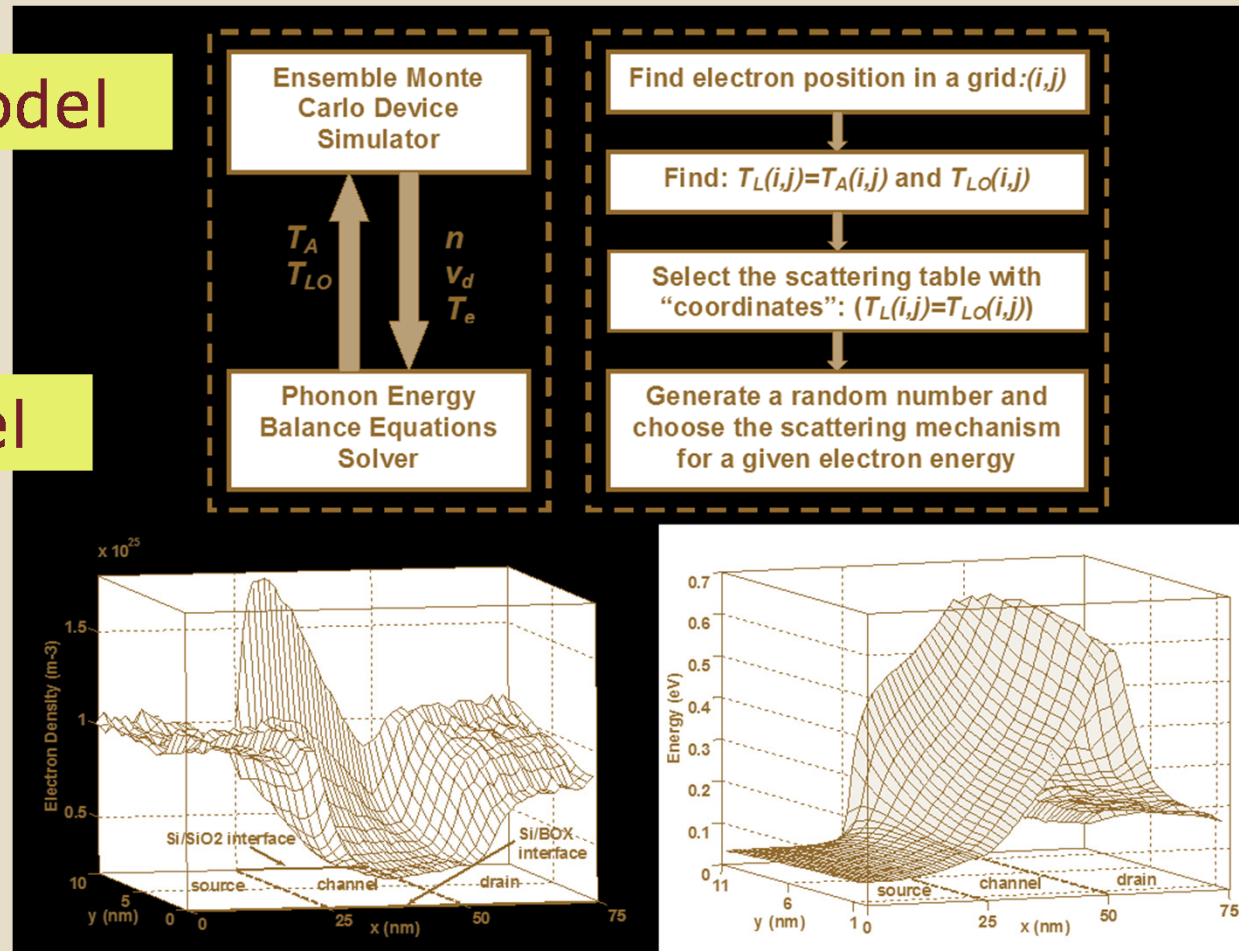
$$C_A \frac{\partial T_A}{\partial t} = \nabla \cdot (k_A \nabla T_A) + C_{LO} \left( \frac{T_{LO} - T_A}{\tau_{LO-A}} \right) + \frac{3nk_B}{2} \left( \frac{T_e - T_L}{\tau_{e-L}} \right).$$

# Exchange of variables between the two kernels

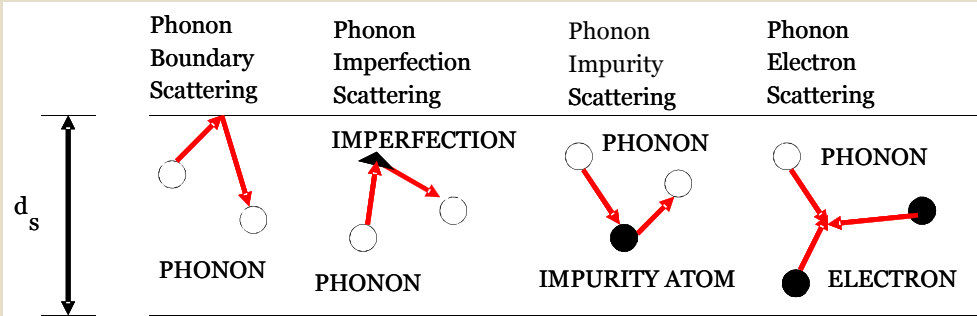


Particle Model

Fluid Model



# Various factors that affect the thermal conductivity value

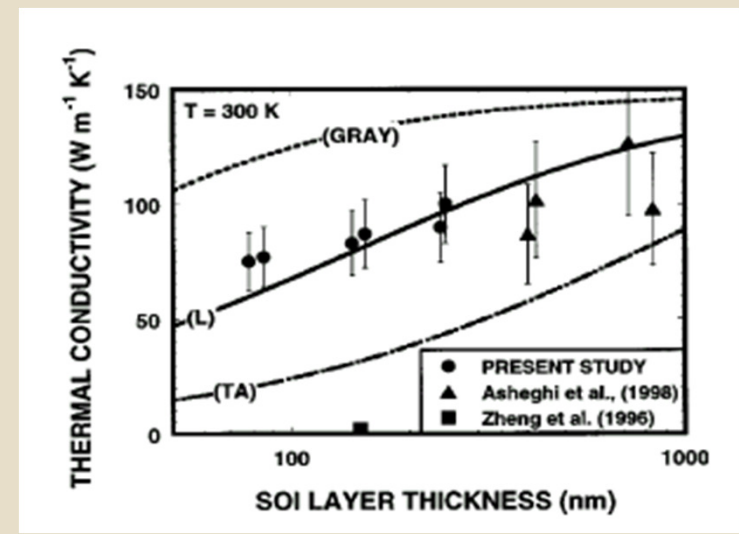
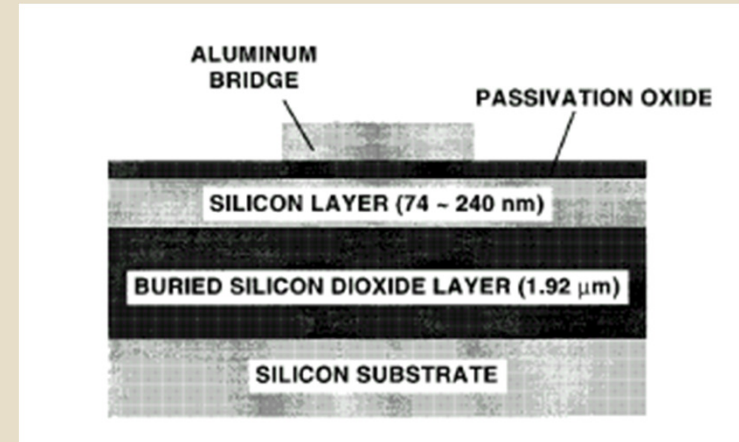
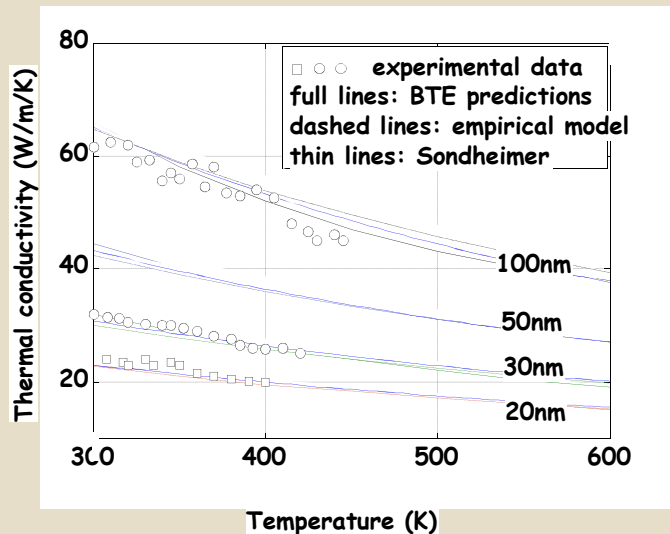


$$\kappa(z) = \kappa_0(T) \int_0^{\pi/2} \sin^3 \theta \left\{ 1 - \exp\left(-\frac{a}{2\lambda(T)\cos\theta}\right) \cosh\left(\frac{a-2z}{2\lambda(T)\cos\theta}\right) \right\} d\theta$$

$$\lambda(T) = \lambda_0(300/T)$$

$$\kappa_0(T) = \frac{135}{a+bT+cT^2} \text{ W/m/K}$$

Vasileska/Raleva Model for the Thermal Conductivity



# Particle-Based Device Simulators



**INCORPORATION OF SPIN**

# Spin-Orbit Effects



- Rashba SO-coupling
- Generating spin polarized currents in nanowires and constrictions
- Band structure in 2DEG
- Transverse Electron Focalization (TEF) in systems with SO-coupling
- Spin accumulation ( Spin Hall Effect in ballistic mesoscopic systems)

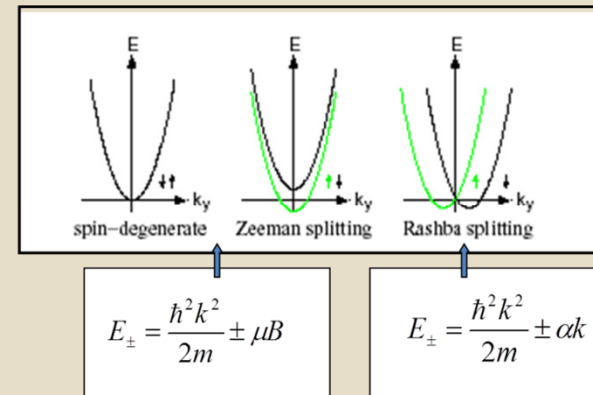
The atomistic effect:

$$M = -\frac{eg}{2mc} S \quad H = -M \cdot B \quad B = \frac{1}{c} v \times E$$

$$H = \frac{eg}{2mc} S \cdot B = -\frac{eg}{2mc^2} S \cdot v \times E = \frac{eg}{2m^2 c^2} S \cdot p \times \nabla \phi(r) \frac{1}{2}$$

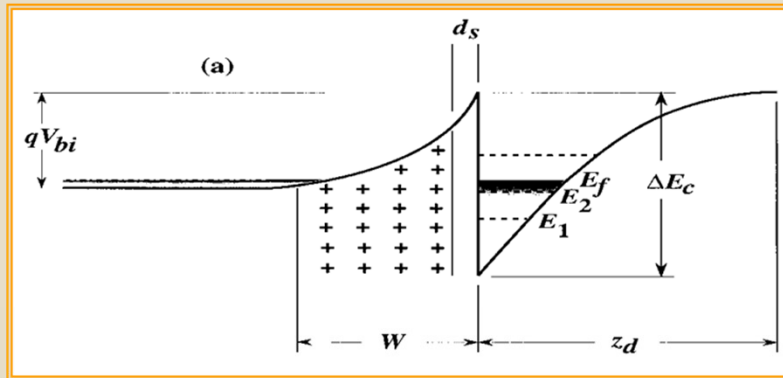
The Thomas precession effect

Heterostructures:



The SO-coupling preserves the time reversal symmetry

# Rashba Spin-Orbit Coupling



$$H_{SO} = - \frac{e\hbar \boldsymbol{\sigma} \cdot \mathbf{p} \times \boldsymbol{\mathcal{E}}}{4m^2 c^2}$$

Rashba spin splitting and Ehrenfest's theorem

R. Winkler\*

Institut für Technische Physik III, Universität Erlangen-Nürnberg, Lst. für Theoretische Festkörperphysik, Staudtstr. 7, D-91058 Erlangen, Germany

Physica E 22 (2004) 450–454

$$H_{SO} = \frac{\alpha}{\hbar} (p_y \sigma_x - p_x \sigma_y)$$

material

Can be controlled with external gates

	$\alpha$
GaAs/AlGaAs	0.5–1 meV nm
InSb/InAlSb	5–10 meV nm

Nitta *et al.* PRL 78 (1997)

Miller *et al.* PRL 90 076807 (2003)

# What are the Proper Transport Models at the Nanoscale?



Semiclassical Transport Approaches

**Quantum Transport**

Atomistic Simulations

**Computational Electronics**



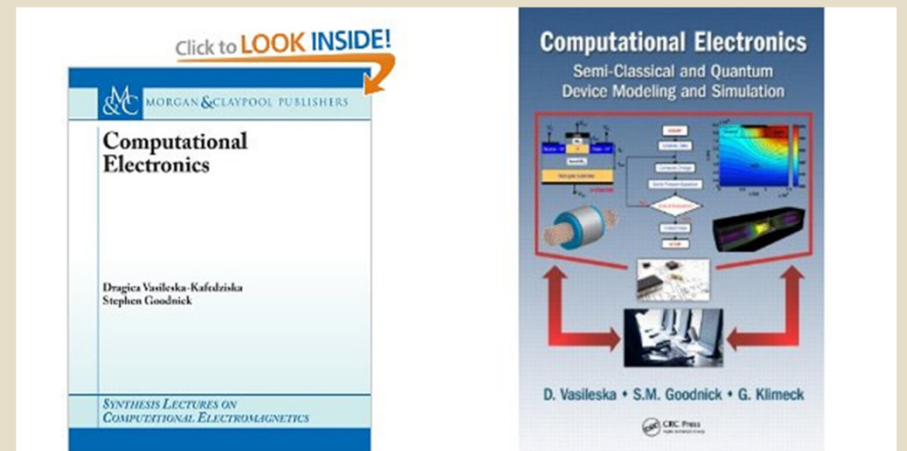
UNIVAC

ENIAC



Grace Hopper – first woman programmer

COMPUTEL





# What do we cover in this section?



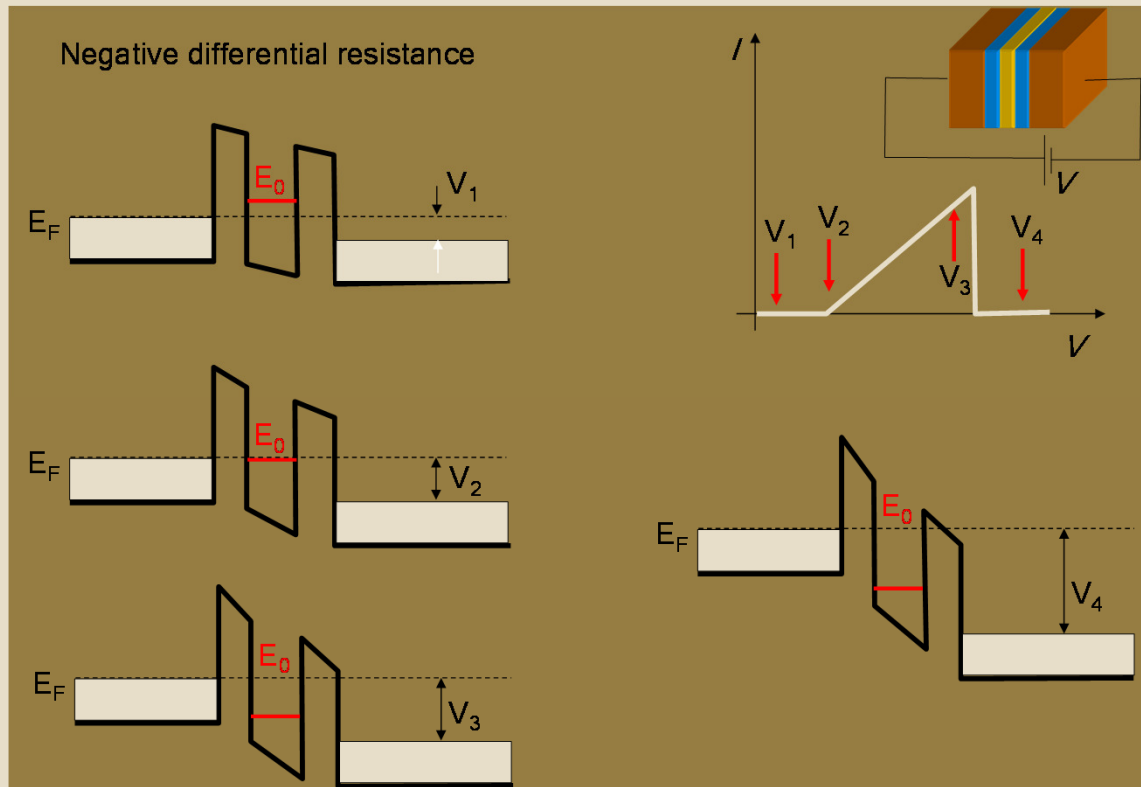
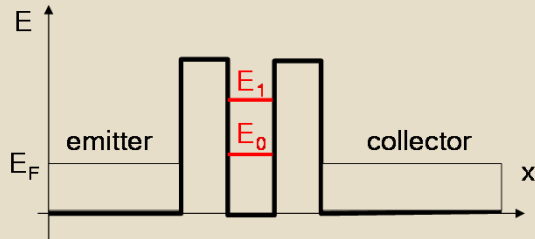
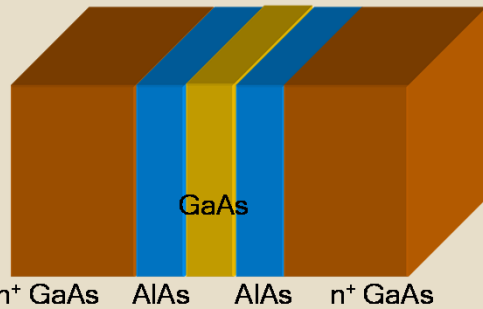
- Quantum Transport
  - ✦ Solution of the Schrodinger Equation Using Usuki Method
  - ✦ Green's Functions
    - Recursive Green's Function Approach
    - Contact Block Reduction Method and its applications

# Quantum Transport

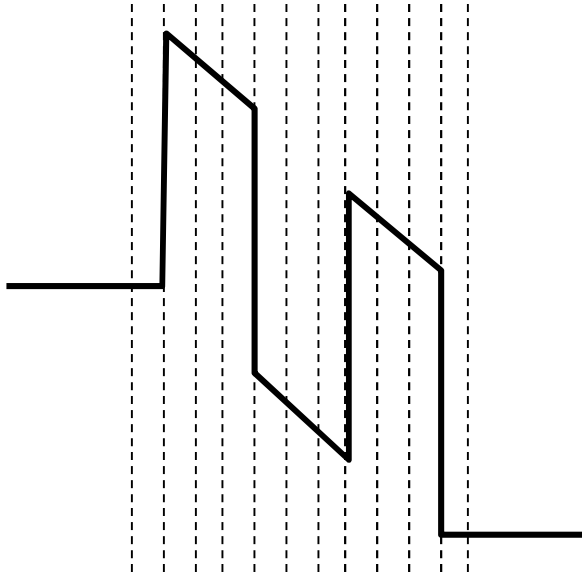


**USUKI METHOD**

# Transfer Matrix Approach on the Example of RTD

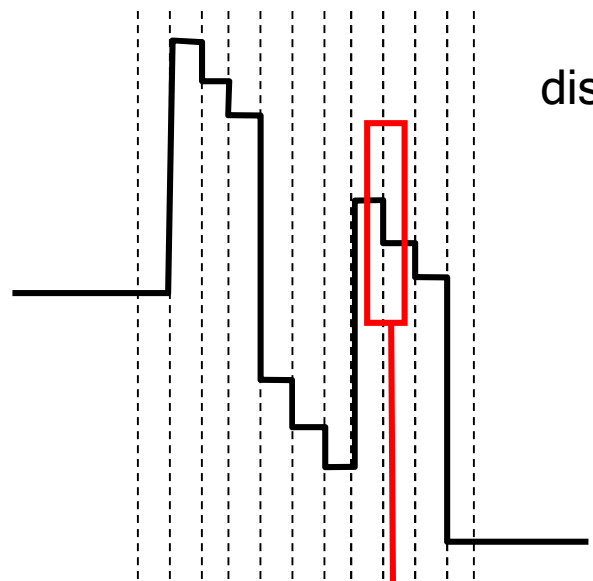


How to calculate the transfer matrix  $T$ ?



divide the active region into N slices

How to calculate the transfer matrix  $T$ ?



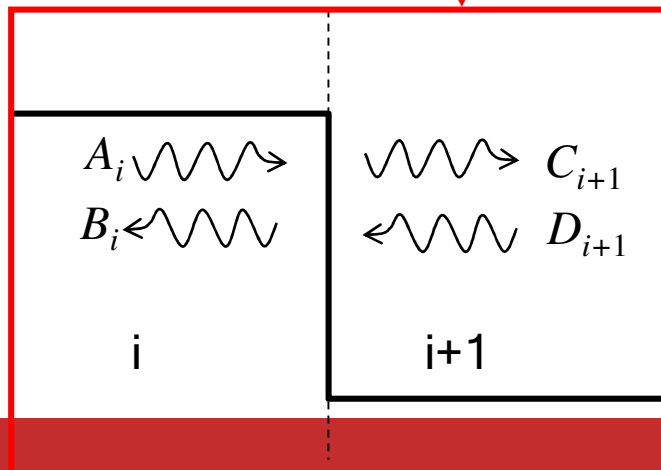
discretize the potential

consider a boundary between slices  $i$  and  $i+1$ :

write down solutions for slices  $i$  and  $i+1$

$$\psi^i(z) = A_i e^{ik_z^i z} + B_i e^{-ik_z^i z}$$
$$\psi^{i+1}(z) = C_{i+1} e^{ik_z^{i+1} z} + D_{i+1} e^{-ik_z^{i+1} z}$$

divide the active region into  $N$  slices

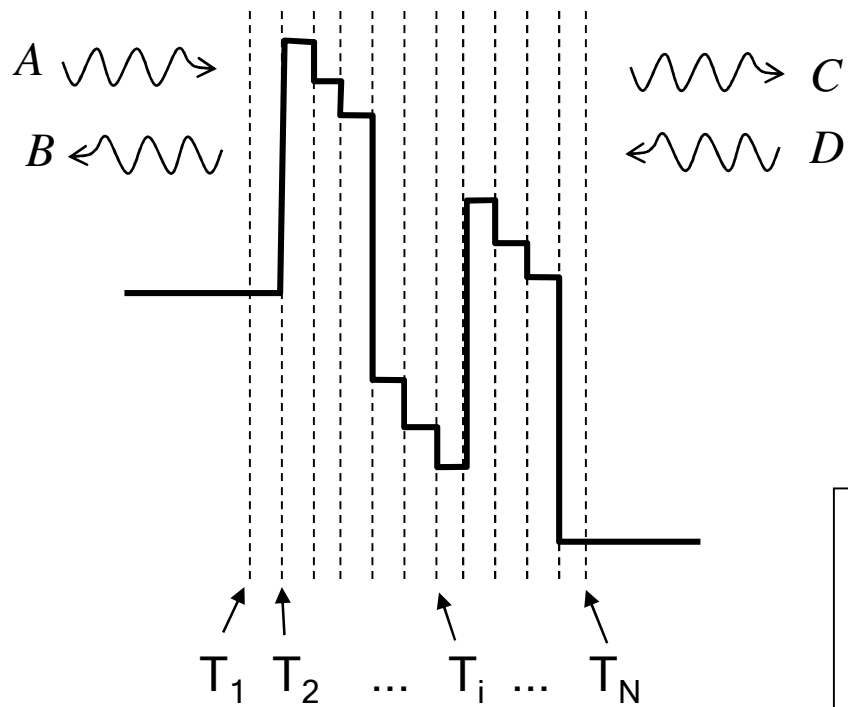


use the continuity conditions

$$\psi^i(z_i) = \psi^{i+1}(z_i)$$
$$\frac{\partial}{\partial z} \psi^i(z_i) = \frac{\partial}{\partial z} \psi^{i+1}(z_i)$$

to calculate transfer matrix  $T_i$  between slices  $i$  and  $i+1$

$$\begin{pmatrix} C_{i+1} \\ D_{i+1} \end{pmatrix} = T_i \begin{pmatrix} A_i \\ B_i \end{pmatrix}$$



total transfer matrix:

$$\begin{pmatrix} C \\ D \end{pmatrix} = T \begin{pmatrix} A \\ B \end{pmatrix}$$

$$T = T_N T_{N-1} \dots T_i \dots T_2 T_1$$

$$T = \begin{pmatrix} 1/t^* & -r^*/t^* \\ -r/t & 1/t \end{pmatrix}$$

Transfer matrix is numerically unstable

Scattering matrix  $S$   
is numerically stable:

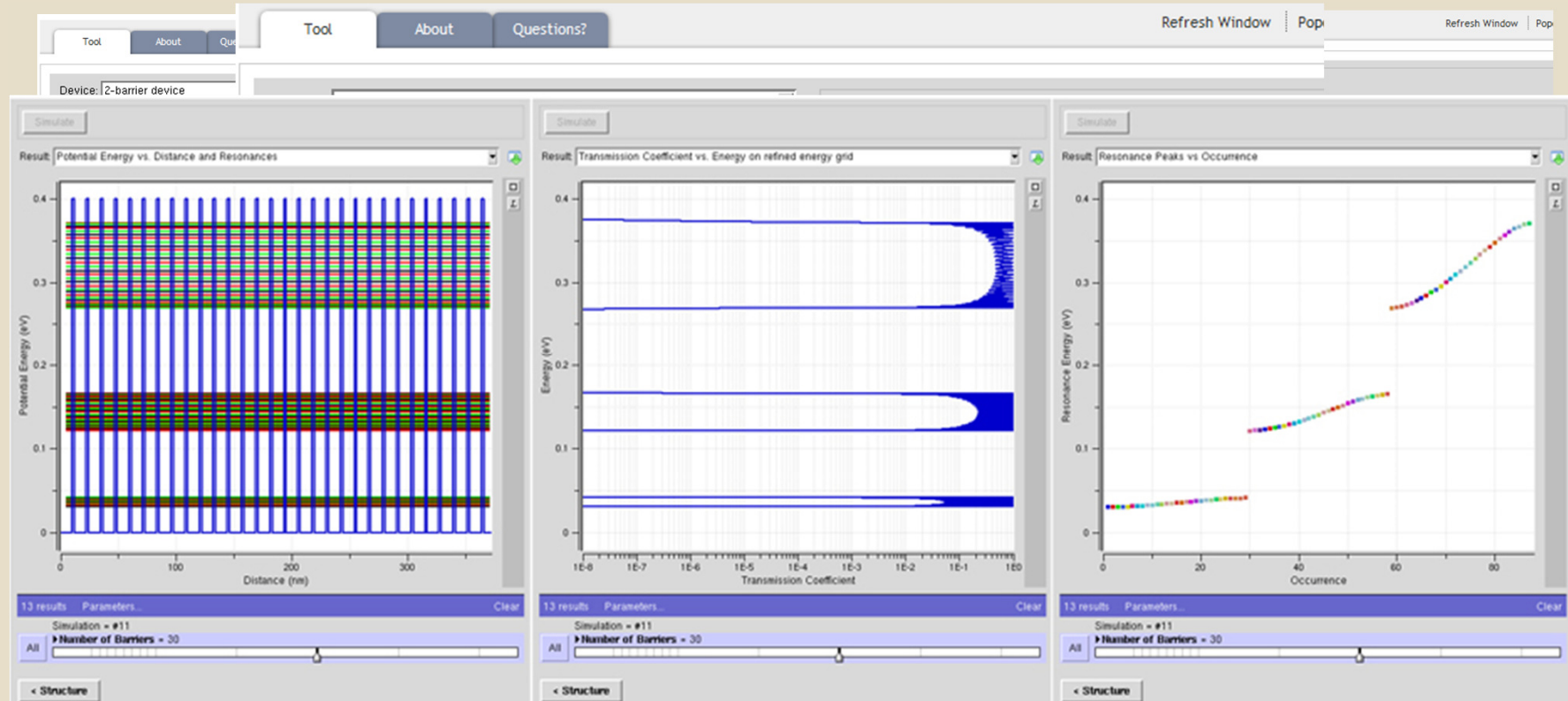
$$\begin{pmatrix} C \\ B \end{pmatrix} = S \begin{pmatrix} A \\ D \end{pmatrix}$$

outgoing states      incoming states

# Exercise for PCPBT



- From one well, to two wells to 5 wells (energy bands formation)

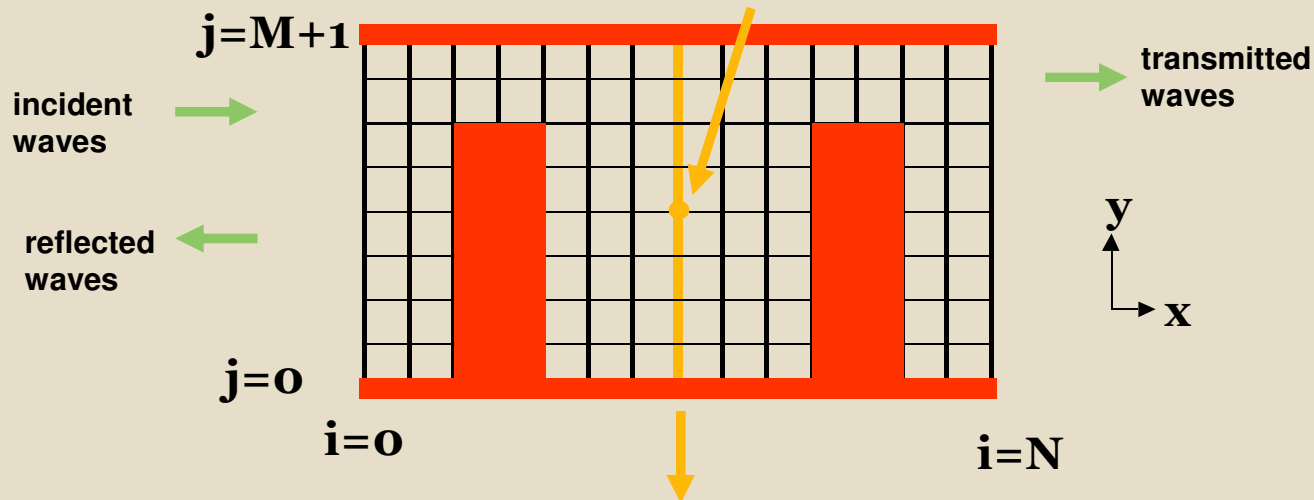


# Usuki Method Explained



Calculate conductance using finite difference grid

Wavefunction and potential defined on discrete grid points  $i, j$



$i$ th slice in x direction - discrete problem involves translating from one slice to the next.

Grid spacing:  $a \ll \lambda_F$



## Obtaining transfer matrices from the discrete SE

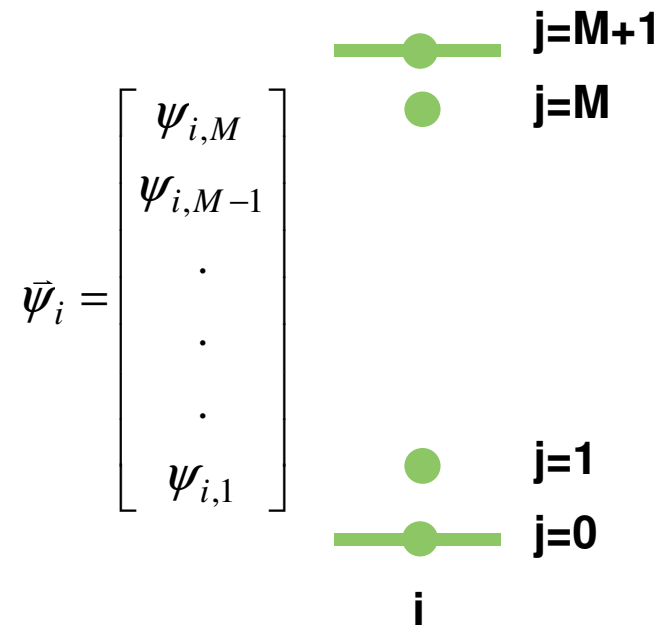
apply Dirichlet boundary conditions on upper and lower boundary:

$$\psi_{i,j=0} = \psi_{i,j=M+1} = 0$$

Wave function on **ith** slice  
can be expressed as a vector 

Discrete SE now becomes a matrix equation  
relating the wavefunction on adjacent slices:

$$(1b) \quad \mathbf{H}_{0i} \vec{\psi}_i - t \vec{\psi}_{i+1} - t \vec{\psi}_{i-1} = E \vec{\psi}_i$$



where:  $\mathbf{H}_{0i} =$

$$\begin{bmatrix} (V_{i,M} + 4t) & -t & 0 & \dots \\ -t & (V_{i,M} + 4t) & -t & \dots \\ \dots & \dots & \dots & \dots \\ \dots & -t & (V_{i,2} + 4t) & -t \\ \dots & 0 & -t & (V_{i,1} + 4t) \end{bmatrix}$$

(1b) can be rewritten as: 
$$\bar{\psi}_{i+1} = \left( \frac{\mathbf{H}_{0i} - E}{t} \right) \bar{\psi}_i - \bar{\psi}_{i-1}$$

Combining this with the trivial equation  $\bar{\psi}_i = \bar{\psi}_i$  one obtains:

$$(2) \quad \begin{bmatrix} \bar{\psi}_i \\ \bar{\psi}_{i+1} \end{bmatrix} = \mathbf{T}_i \begin{bmatrix} \bar{\psi}_{i-1} \\ \bar{\psi}_i \end{bmatrix}$$

where 
$$\mathbf{T}_i = \begin{bmatrix} 0 & -\mathbf{I} \\ -\mathbf{I} & \left( \frac{\mathbf{H}_{0i} - E}{t} \right) \end{bmatrix}$$
 Is the transfer matrix relating adjacent slices

Modification for a perpendicular magnetic field (0,0,B) :

$$\mathbf{T}_i = \begin{bmatrix} 0 & -\mathbf{I} \\ -\mathbf{P}^2 & \left( \frac{\mathbf{P}(\mathbf{H}_{0i} - E)}{t} \right) \end{bmatrix}$$

B enters into phase factors  
important quantity:  
flux per unit cell



$$P_{i,j} = e^{i2\pi\beta j} \delta_{i,j},$$

$$\beta = \frac{Ba^2}{h/e} = \varphi / \varphi_0$$

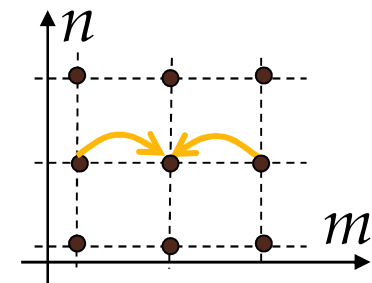
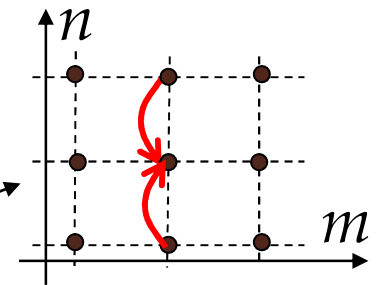
# An aside – how the Peierl's substitution appears in a tight-binding Hamiltonian

$$\mathbf{k} \rightarrow -i\nabla - e\mathbf{A}/\hbar, \quad \Psi \rightarrow \Psi \exp(-i 2\pi \mathbf{A} \cdot \mathbf{r}/\phi_0),$$

$$H = \sum_{m,n} |m,n\rangle (\epsilon_0 + V_{mn}) \langle m,n| + t |m,n\rangle (\langle m,n+1| + \langle m,n-1|) +$$

$$+ t |m,n\rangle \left( e^{iBa^2n/\hbar} \langle m+1,n| + e^{-iBa^2n/\hbar} \langle m-1,n| \right)$$

magnetic field (Peierls substitution)



**Solving the eigenvalue problem:**  $\mathbf{T}_1 \begin{bmatrix} \bar{\psi}_1 \\ \bar{\psi}_0 \end{bmatrix} = \lambda \begin{bmatrix} \bar{\psi}_1 \\ \bar{\psi}_0 \end{bmatrix}$  **yields the modes on the left side of the system**

**Mode eigenvectors have the generic form:**  $\begin{bmatrix} \bar{u}_m(\pm) \\ \lambda_m(\pm)\bar{u}_m(\pm) \end{bmatrix}$  **← redundant**

**There will be M modes that propagates to the right (+) with eigenvalues:**  
**propagating**

$$\lambda_m(+)=e^{ik_m a}, m=1, \dots, q$$

$$\lambda_m(+)=e^{-\kappa_m a}, m=q+1, \dots, M$$

**evanescent**

**There will be M modes that propagates to the left (-) with eigenvalues:**

$$\lambda_m(-)=e^{-ik_m a}, m=1, \dots, q$$

**propagating**

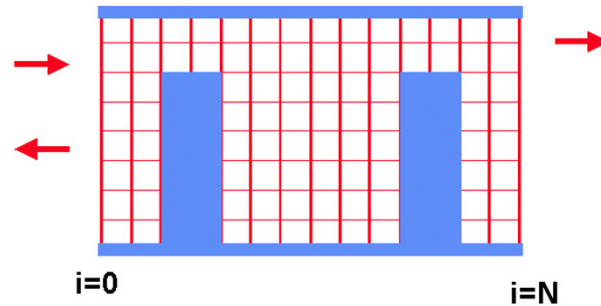
$$\lambda_m(-)=e^{\kappa_m a}, m=q+1, \dots, M$$

**evanescent**

**defining**  $\mathbf{U}_{\pm} = [\bar{u}_1(\pm) \ \dots \ \bar{u}_m(\pm)]$  **and**  $\lambda_{\pm} = \text{diag}[\lambda_1(\pm) \ \dots \ \lambda_m(\pm)]$

**Complete matrix of eigenvectors:**  $\mathbf{U}_{\text{tot}} = \begin{bmatrix} \mathbf{U}_+ & \mathbf{U}_- \\ \lambda_+ \mathbf{U}_+ & \lambda_- \mathbf{U}_- \end{bmatrix}$

# Transfer matrix equation for translation across entire system



Transmission matrix

Unit matrix  
waves incident  
from left have unit  
amplitude

Zero matrix  
no waves incident  
from right

$$\begin{bmatrix} \mathbf{t} \\ \mathbf{0} \end{bmatrix}$$

$$= \mathbf{U}_{tot}^{-1} \mathbf{T}_{N-1} \mathbf{T}_{N-2} \cdots \mathbf{T}_1 \mathbf{U}_{tot}$$

$$\begin{bmatrix} \mathbf{I} \\ \mathbf{r} \end{bmatrix}$$

reflection  
matrix

Converts back to  
mode basis

Converts from mode basis  
to site basis

Recall:

$$G = \frac{2e^2}{h} \sum_{m,n} \frac{v_n}{v_m} |t_{n,m}|^2$$



In general, the velocities must  
be determined numerically

Variation on the cascading scattering matrix technique method  
 Usuki et al. Phys. Rev. B 52, 8244 (1995)

Boundary condition- waves of unit amplitude incident from right

$$\longrightarrow \mathbf{C}_1^{(0,0)} = \mathbf{I}, \mathbf{C}_2^{(0,0)} = \mathbf{0}$$

Iteration scheme for interior slices

$$\begin{bmatrix} \mathbf{C}_1^{(i+1,0)} & \mathbf{C}_2^{(i+1,0)} \\ \mathbf{0} & \mathbf{I} \end{bmatrix} = \mathbf{T}_i \begin{bmatrix} \mathbf{C}_1^{(i,0)} & \mathbf{C}_2^{(i,0)} \\ \mathbf{0} & \mathbf{I} \end{bmatrix} \mathbf{P}_i$$

$$\mathbf{P}_i = \begin{bmatrix} \mathbf{I} & \mathbf{0} \\ \mathbf{P}_{i1} & \mathbf{P}_{i2} \end{bmatrix},$$

$$\mathbf{P}_{i1} = -\mathbf{P}_{i2} \mathbf{T}_{i21} \mathbf{C}_1^{(i,0)},$$

$$\mathbf{P}_{i2} = [\mathbf{T}_{i21} \mathbf{C}_2^{(i,0)} + \mathbf{T}_{i22}]^{-1}$$

plays an analogous role to Dyson's equation in Recursive Greens Function approach

Final transmission matrix for entire structure is given by

$$\mathbf{t} = -(\mathbf{U}^+ \lambda^+)^{-1} \left[ \mathbf{C}_1^{N+1} - \mathbf{U}^+ (\mathbf{U}^+ \lambda^+)^{-1} \right]^{-1}$$

A similar iteration gives the reflection matrix

**After the transmission problem has been solved,  
the wave function can be reconstructed**

**It can be shown that:**

$$\mathbf{P}_{N2} = \Psi_N = \left[ \vec{\psi}_{N,1} \quad \cdots \quad \vec{\psi}_{N,k} \quad \cdots \quad \vec{\psi}_{N,M} \right]$$



**wave function on column N resulting from the *k*th mode**

**One can then iterate  
backwards through the structure:**  $\Psi_i = \mathbf{P}_{i1} + \mathbf{P}_{i2} \Psi_{i+1}$

**The electron density at each point is then given by:**

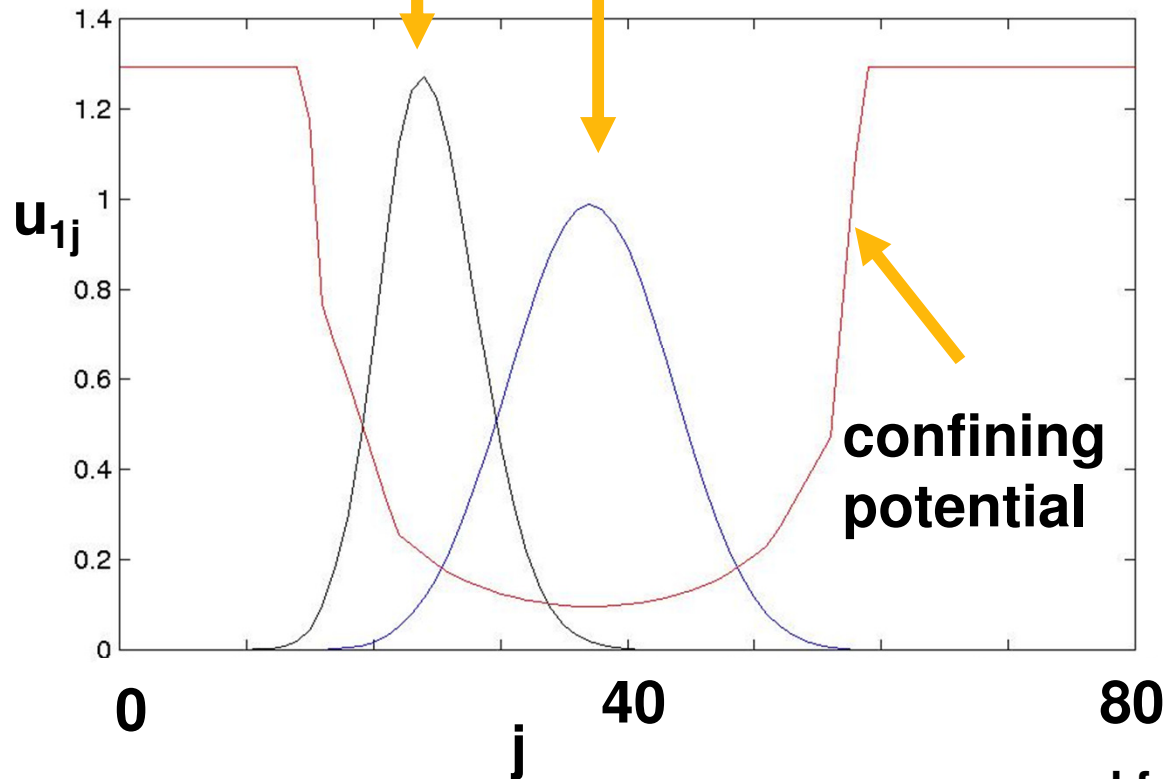
$$n(x, y) = n(i, j) = \sum_{k=1}^q \left| \psi_{ijk} \right|^2$$



# First propagating mode for an irregular potential

$\vec{u}_1(+)$  for  $B=0.7$  T

$\vec{u}_1(+)$  for  $B=0$  T



$$\vec{u}_n \equiv \varphi_n(y)$$

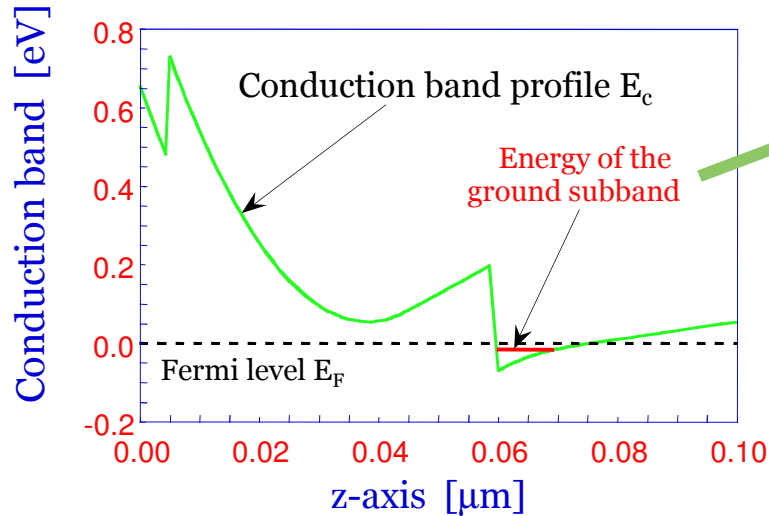
Mode functions no longer simple sine functions

$$v_m = \frac{e}{h} \sum_j 2t \sin(2k_m - 2\pi\beta j) u_{mj}^2$$

general formula for velocity of mode  $m$  obtained by taking the expectation value of the velocity operator with respect to the basis vector.



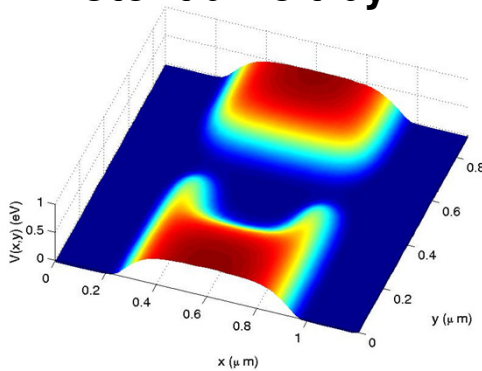
# Example – Quantum Dot Conductance as a Function of Gate voltage



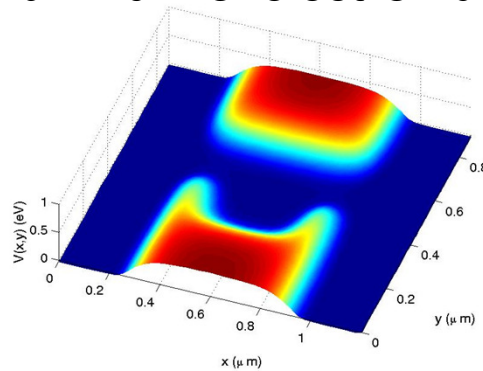
Simulation gives comparable 2D electron density to that measured experimentally

$$N = \frac{\hbar^2}{2m^*} (E_F^{3D} - E_0) \sim 4 \times 10^{11} \text{ cm}^{-2}$$

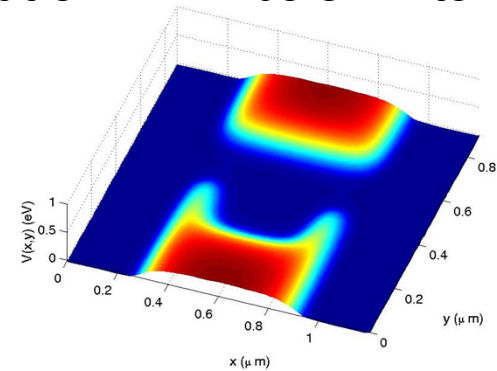
Potential felt by 2DEG- maximum of electron distribution ~7nm below interface



$V_g = -1.0 \text{ V}$

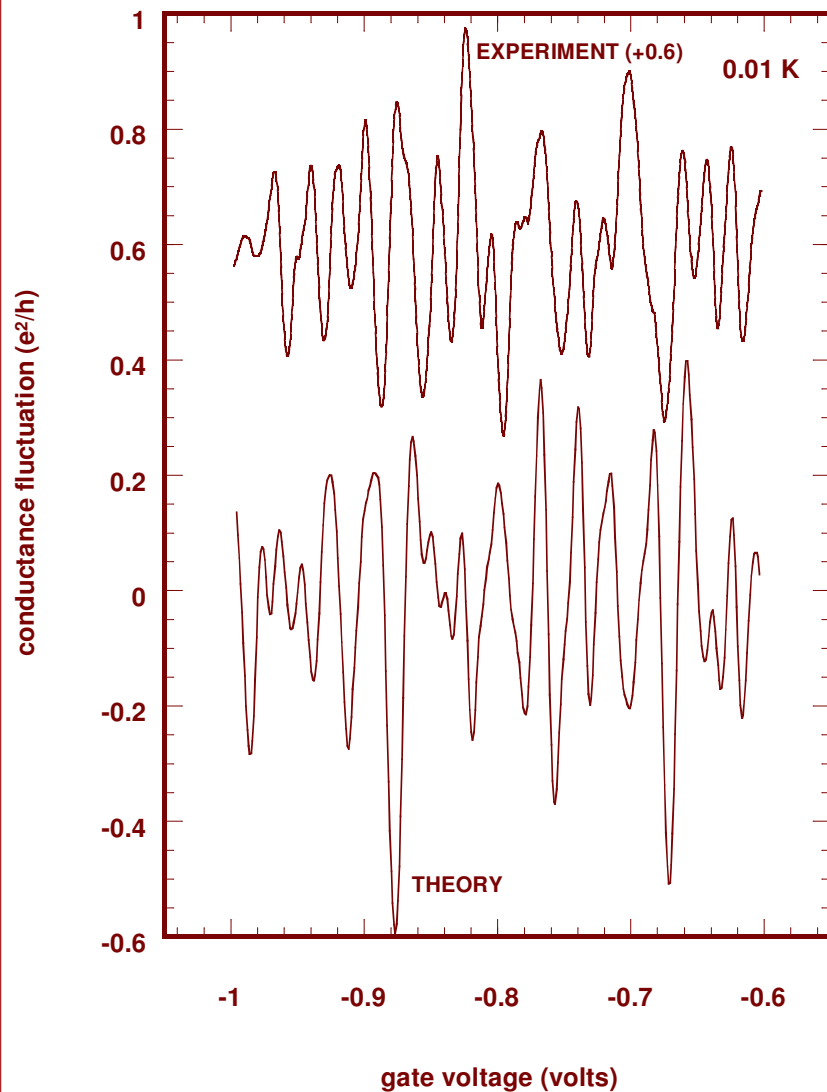


$V_g = -0.9 \text{ V}$



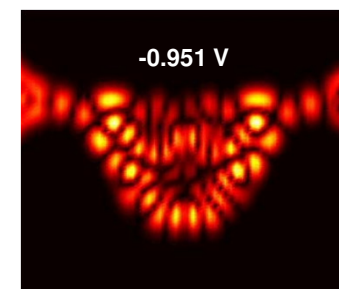
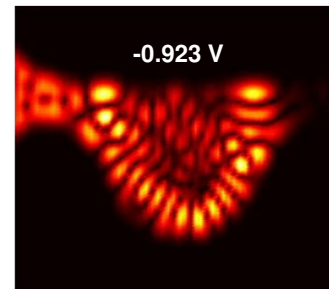
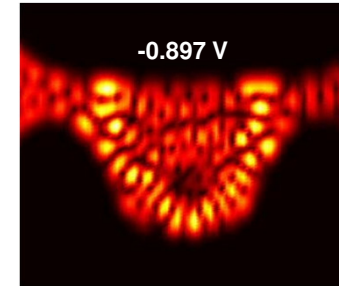
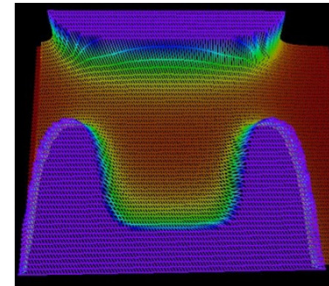
$V_g = -0.7 \text{ V}$

Potential evolves smoothly- calculate a few as a function of  $V_g$ , and create the rest by interpolation



Subtracting out a background that removes the underlying steps you get periodic fluctuations as a function of gate voltage.

Theory and experiment agree very well



Same simulations also reveal that certain scars may **RECUR** as gate voltage is varied. The resulting periodicity agrees **WELL** with that of the conductance oscillations

\* Persistence of the scarring at zero magnetic field indicates its **INTRINSIC** nature

⇒ The scarring is **NOT** induced by the application of the magnetic field

# Quantum Transport



**RECURSIVE GREEN'S FUNCTIONS APPROACH**



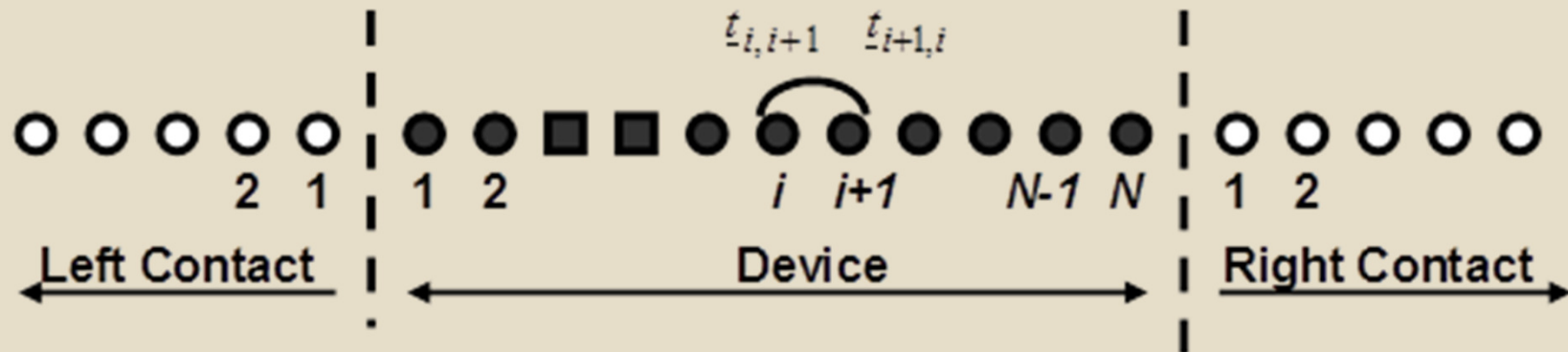


# Matrix Representation of the Kinetic Equations



$$\left[ \underline{EI} - \underline{H} - \underline{\Sigma}_B^r - \underline{\Sigma}_{Scat}^r \right] \underline{G}^r = \underline{I}$$

$$\underline{G}^{>,<} = \underline{G}^r \left( \underline{\Sigma}_B^{>,<} + \underline{\Sigma}_{Scat}^{>,<} \right) \underline{G}^a$$

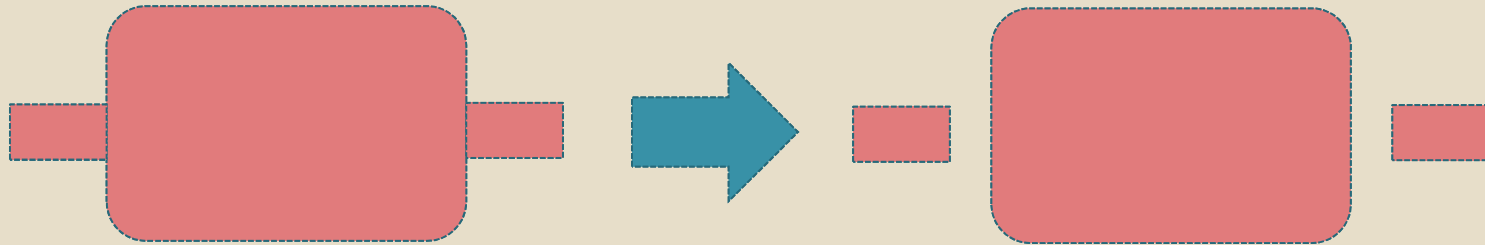


[K. B. Kahen](#), Recursive-Green's-function analysis of wave propagation in two-dimensional nonhomogeneous media, .Phys. Rev. E 47, 2927 - 2933 (1993).

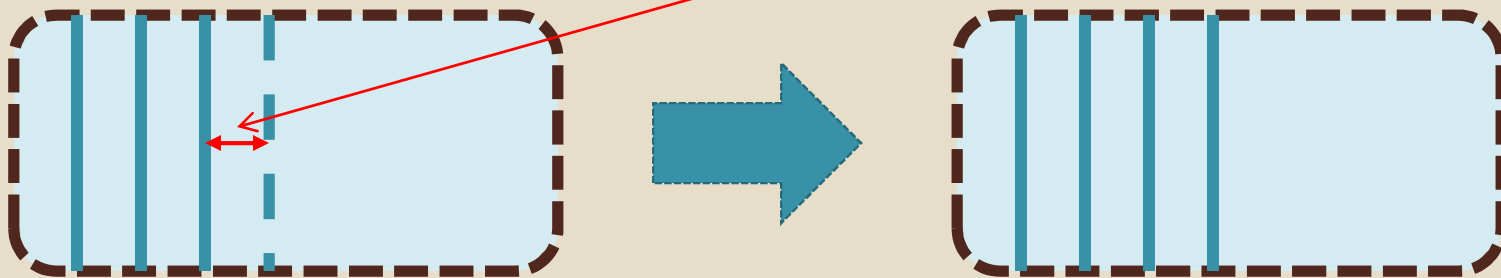
# Recursive Green's Function Method at Work



1. Divide the system into leads and internal domain



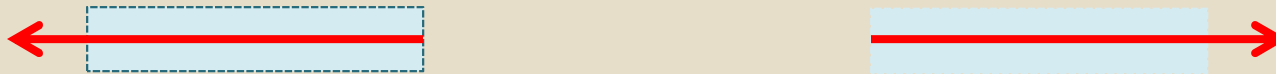
2. Calculate the Green's Function of the internal structure using the Dyson Equation  $g = g^0 + g^0 V g$



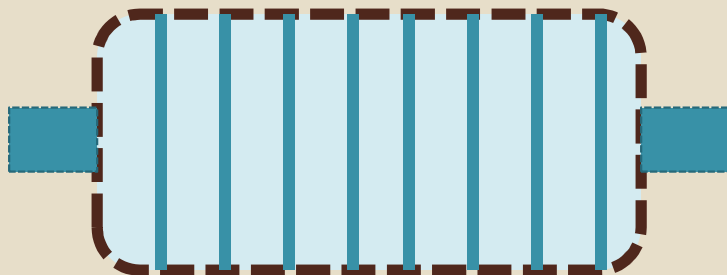
# Recursive Green's Function Method at Work



3. Calculate Green's functions of the semi-infinite leads  $\rightarrow$  Surface Green's function (self energy)



4. Use the Dyson Equation to connect the two domains of the system



$$g_{L_{1,1}}^{r\nu} = \frac{A_{L_1}^2 + t_1^2 - t_2^{\nu^2} - \sqrt{\left[A_{L_1}^2 + t_1^2 - t_2^{\nu^2}\right]^2 - 4A_{L_1}^2 t_1^2}}{2A_{L_1}^2 t_1^2}$$

$$\Sigma_L^{r\nu} = t_1^2 g_{L_{1,1}}^{r\nu}$$

# Recursive Green's Function Method at Work



Left-connected  
Green's function:

$$\underline{A}_{1,1} \underline{g}_{1,1}^{Lr} = \underline{I}_{1,1} \quad \underline{A} = \left[ \underline{E} \underline{I} - \underline{H} - \underline{\Sigma}^r \right]$$

$$\underline{g}_{q+1,q+1}^{Lr} = \left( \underline{A}_{q+1,q+1} - \underline{A}_{q+1,q} \underline{g}_{q,q}^{Lr} \underline{A}_{q,q+1} \right)^{-1}$$

Right-connected  
Green's function:

$$\underline{A}_{N,N} \underline{g}_{N,N}^{Rr} = \underline{I}_{N,N}$$

$$\underline{g}_{q-1,q-1}^{Rr} = \left( \underline{A}_{q-1,q-1} - \underline{A}_{q-1,q} \underline{g}_{q,q}^{Rr} \underline{A}_{q,q-1} \right)^{-1}$$

Green's functions needed  
for transmission coefficient  
and electron density  
calculations

$$\underline{G}_{q,q}^r = \underline{g}_{q,q}^{Lr} + \underline{g}_{q,q}^{Lr} \left( \underline{A}_{q,q+1} \underline{G}_{q+1,q+1}^r \underline{A}_{q+1,q} \right) \underline{g}_{q,q}^{Lr}$$

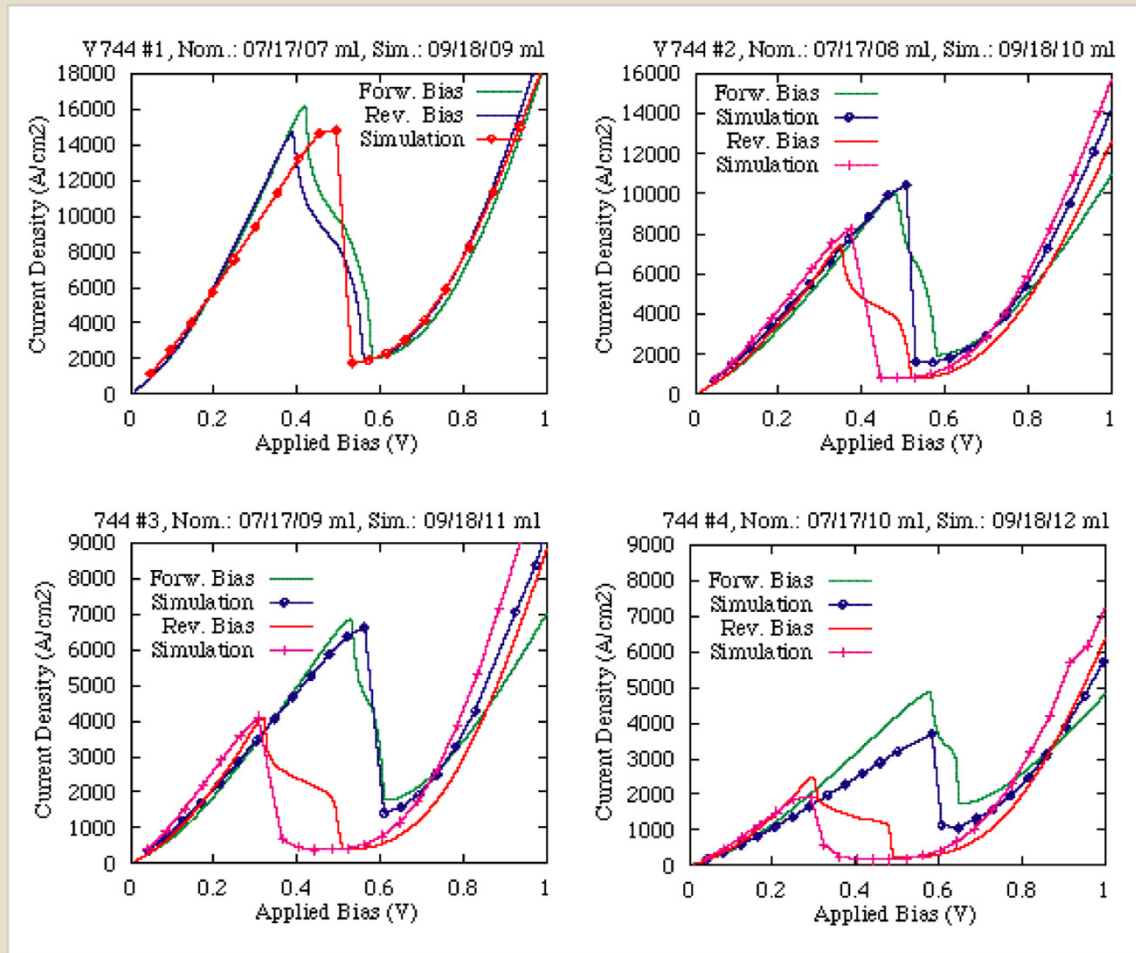
$$\underline{G}_{q+1,q+1}^r = \underline{g}_{q+1,q+1}^{Rr} + \underline{g}_{q+1,q+1}^{Rr} \left( \underline{A}_{q+1,q} \underline{G}_{q,q}^r \underline{A}_{q,q+1} \right) \underline{g}_{q,q}^{Rr}$$



# Example: Simulation of a RTD with NEMO1D



## NEMO1D: InGaAs/AlAs RTDs

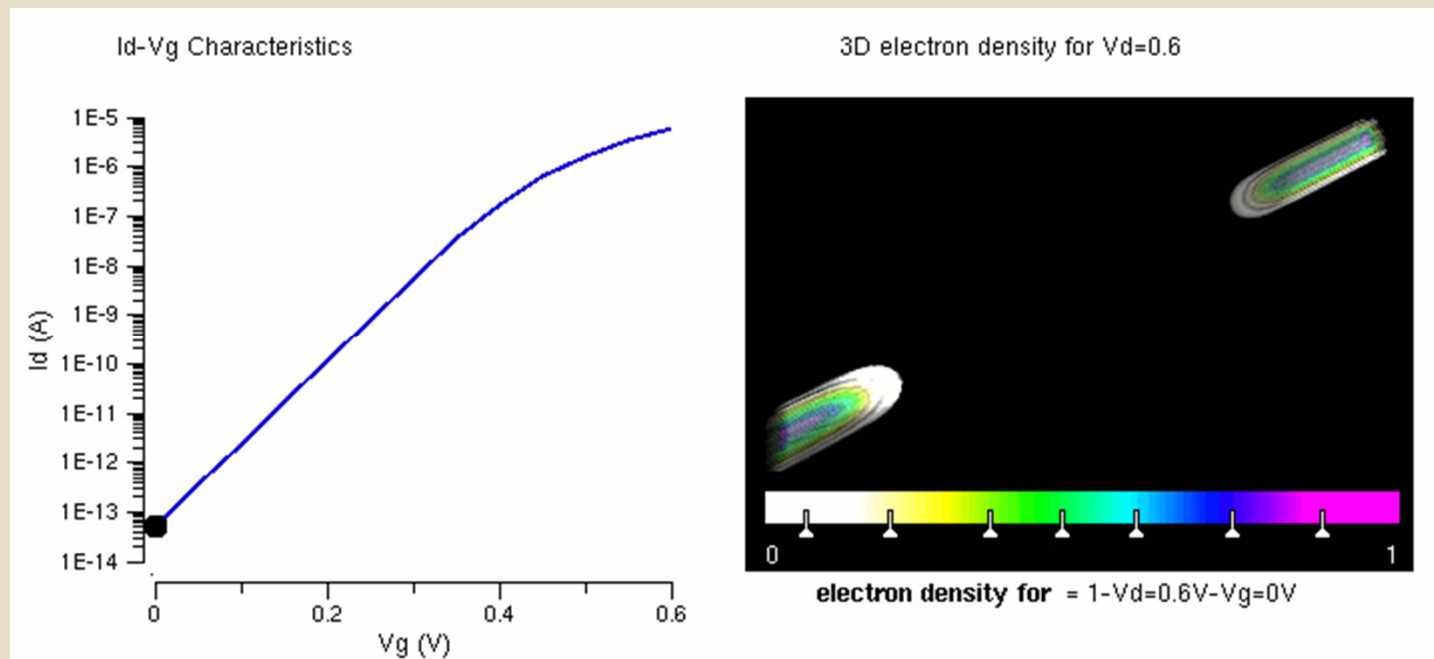


G. Klimeck, private communication..

# Example: Simulation of a Nanowire MOSFET with OMEN



## OMEN: Modeling of Nanowire Transistors



Simulation result for formation of inversion channel (electron density) and attainment of threshold voltage (IV) in a nanowire MOSFET. Note that the threshold voltage for this device lies around 0.45V

# Quantum Transport



## **CONTACT BLOCK REDUCTION METHOD**



# Direct Solution of the Problem is Time Consuming



The retarded Green's function of an open system:

$$\mathbf{G}^R(E) = [\mathbf{I}E - \mathbf{H}]^{-1} = [\mathbf{I}E - \mathbf{H}^0 - \Sigma]^{-1}$$

where  $\mathbf{H}^0 \Rightarrow$  closed system Hamiltonian ,  $\Sigma \Rightarrow$  self-energy matrix

The Dyson equation,

$$\mathbf{G}^R(E) = [\mathbf{I} - \mathbf{G}^0(E)\Sigma(E)]^{-1} \mathbf{G}^0(E),$$

where  $\mathbf{G}^0(E) \equiv [\mathbf{I}E - \mathbf{H}^0 + i\eta]^{-1} = \sum_{\alpha} \frac{|\alpha\rangle\langle\alpha|}{E - \varepsilon_{\alpha} + i\eta} \Big|_{\eta=0^+}$ ,  $\mathbf{H}^0|\alpha\rangle = E_{\alpha}|\alpha\rangle$

$\mathbf{G}^0(E)$  describes closed system (decoupled device)

**To determine Green's function of an open system  
we need to invert a huge matrix**

D. Mamaluy, D. Vasileska, M. Sabathil, T. Zibold, and P. Vogl, "Contact block reduction method for ballistic transport and carrier densities of open nanostructures", Phys. Rev. B 71, 245321 (2005).

# The CBR Algorithm



$\mathbf{G}^R$  of an open system in CBR formalism:

$$\mathbf{G}^R = \begin{bmatrix} \mathbf{G}_C^R & \mathbf{G}_{CD}^R \\ \mathbf{G}_{DC}^R & \mathbf{G}_D^R \end{bmatrix} = \begin{bmatrix} \mathbf{A}_C^{-1} \mathbf{G}_C^0 & \mathbf{A}_C^{-1} \mathbf{G}_{CD}^0 \\ -\mathbf{A}_{DC} \mathbf{A}_C^{-1} \mathbf{G}_C^0 + \mathbf{G}_{DC}^0 & -\mathbf{A}_{DC} \mathbf{A}_C^{-1} \mathbf{G}_{CD}^0 + \mathbf{G}_D^0 \end{bmatrix},$$

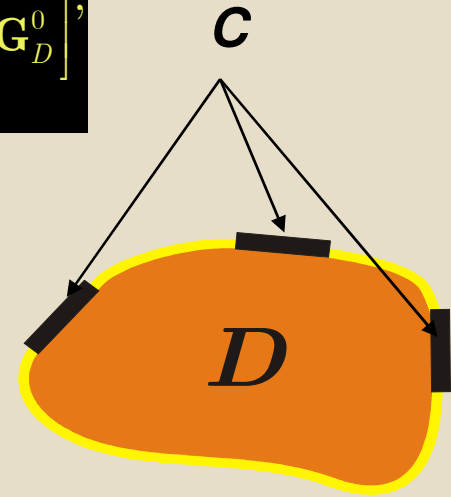
$$\mathbf{A}_C = \mathbf{1}_C - \mathbf{G}_C^0 \boldsymbol{\Sigma}_C, \mathbf{A}_{DC} = -\mathbf{G}_{DC}^0 \boldsymbol{\Sigma}_C$$

$\mathbf{G}_C^0$  is the contact portion of the  $\mathbf{G}^0$

where,

index  $D$  denotes the interior device region

index  $C$  denotes the contact ( boundary ) region



All elements of  $\mathbf{G}^R$  can be determined from inversion of small matrix  $\mathbf{A}_C$

- The left upper block  $\mathbf{G}_C^R$  fully determine the transmission function
- The left lower block  $\mathbf{G}_{DC}^R$  determines density of states, charge density etc.

# Transmission Coefficient and Electron Density



- Transmission Function

$$T_{\lambda\lambda'}(E) = \text{Tr}(\Gamma^\lambda \mathbf{G}^R \Gamma^{\lambda'} \mathbf{G}^{R\dagger})$$

- CBR Formalism

$$T_{\lambda\lambda'}(E) = \text{Tr}(\Gamma_C^\lambda \mathbf{G}_C^R \Gamma_C^{\lambda'} \mathbf{G}_C^{R\dagger}), \text{ where } \mathbf{G}_C^R = [\mathbf{1} - \mathbf{G}_C^0 \Sigma_C]^{-1} \mathbf{G}_C^0 \quad \Gamma_C^\lambda = i[\Sigma_C - \Sigma_C^\dagger]$$

- Local Density of States Function

$$\rho(\mathbf{r}, E) = \langle \mathbf{r} | \mathbf{G}^R \Gamma \mathbf{G}^{R\dagger} | \mathbf{r} \rangle / 2\pi$$

- CBR Formalism

$$\rho(\mathbf{r}, E) = \frac{1}{2\pi} \sum_m |\mathbf{G}_{\mathbf{r}m}^R|^2 \Gamma_{mm},$$

$$\mathbf{G}_{\mathbf{r}m}^R = \langle \mathbf{r} | \mathbf{G}_{DC}^0 \mathbf{B}_C^{-1} | m \rangle = \sum_{m', \alpha} \frac{\langle \mathbf{r} | \alpha \rangle \langle \alpha | m' \rangle}{E - \varepsilon_\alpha + i\eta} \Big|_{\eta=0^+} \langle m' | \mathbf{B}_C^{-1} | m \rangle$$

# Complexity of CBR vs. Other Algorithms



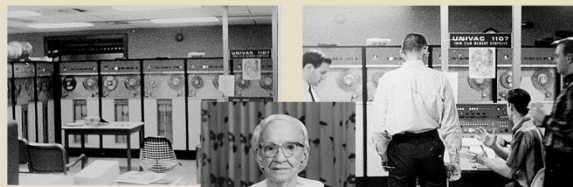
Method	Computational cost
Transfer matrix + QTBM	$N_E \times O(N_{TOTAL}^3)$
NanoMOS (Purdue University)	$N_E \times N_x \times O([N_y N_z]^2) \approx N_E \times O(N_{TOTAL}^{5/3})$
QDAME (IBM, S. Laux)	$N_{TOTAL} \times O(N_{eigen}^2) + N_E \times O(N_{TOTAL}^{3/2})$
CBR	$N_{TOTAL} \times O(N_{eigen}^2) + N_E \times O(N_{TOTAL})$
<b>Notations</b>  $N_E$ : number of energy steps;  $N_{TOTAL}$ : number of grid points  $N_{eigen}$ : number of eigenvalues	<b>CBR WINS !!!</b>

# What are the Proper Transport Models at the Nanoscale?



Semiclassical Transport Approaches  
Quantum Transport  
**Atomistic Simulations**

## Computational Electronics



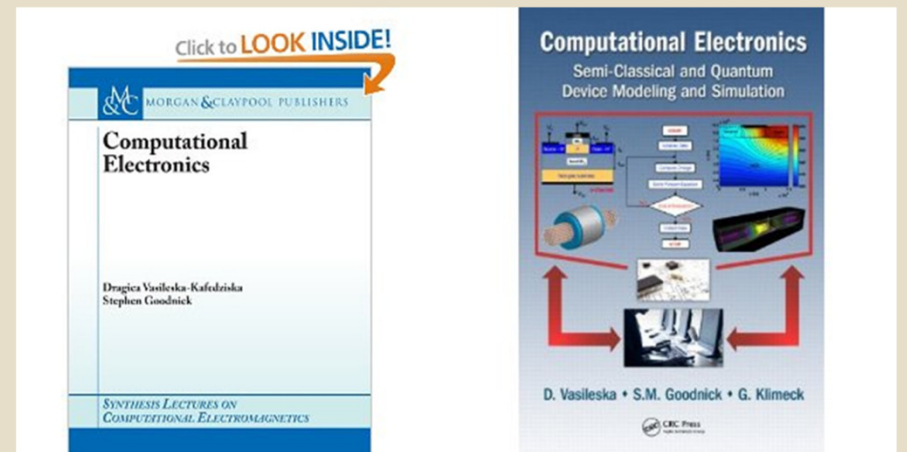
UNIVAC

ENIAC



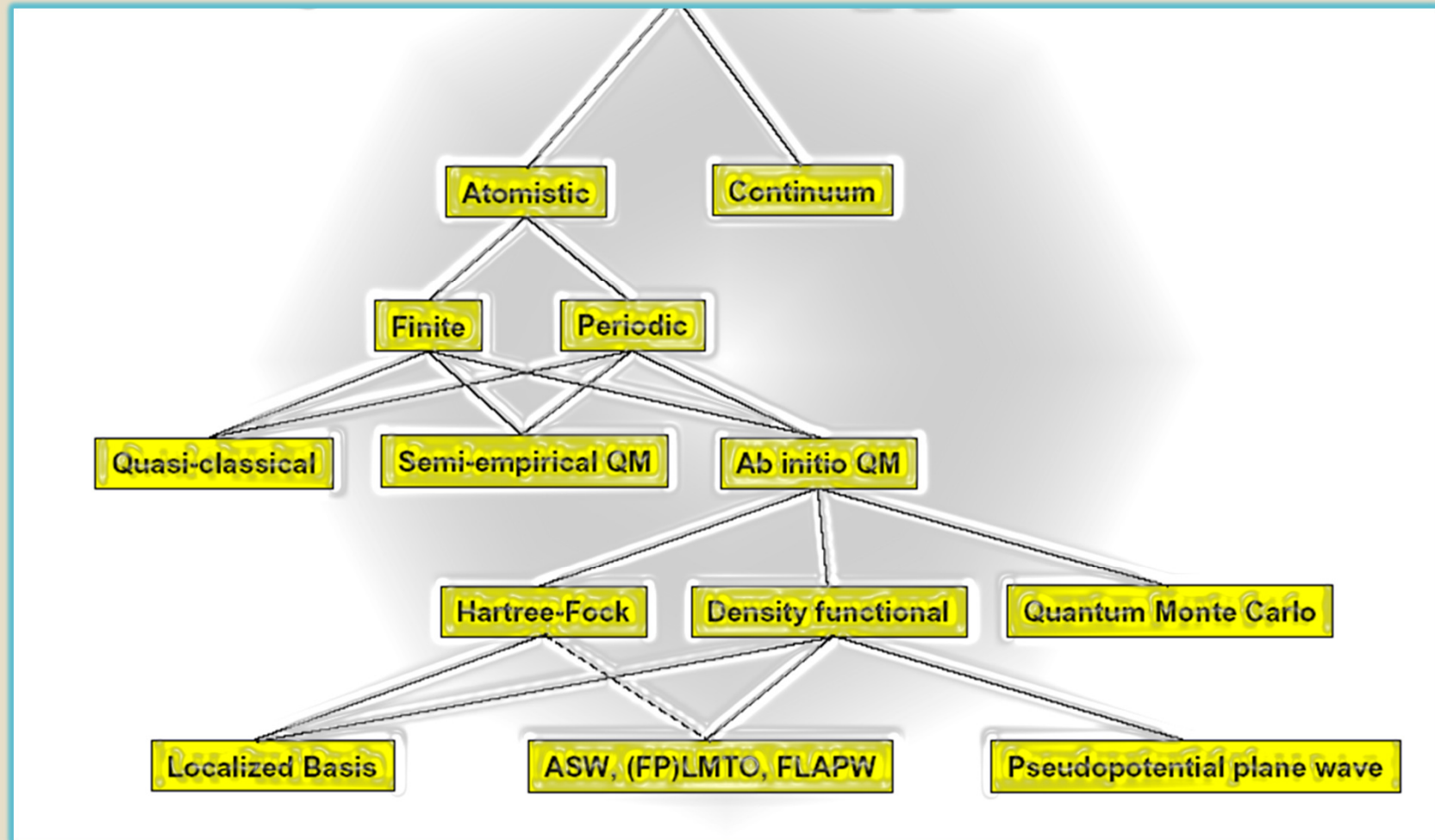
Grace Hopper – first woman programmer

COMPUTEL





# First Principles Calculations

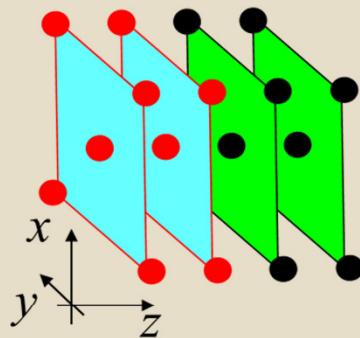


# Self-Consistent Tight Binding Calculations



[A. Di Carlo et. al., Solid State Comm. 98, 803 (1996); APL 74, 2002 (1999)]

The electron and hole densities in each 2D layer are given by:



$$n(z) = \frac{1}{(2\pi)^2} \int_{BZ_{\parallel}} d^2\mathbf{k}_{\parallel} \sum_c |\langle z | E_c \mathbf{k}_{\parallel} \rangle|^2 f(E_c - F_n)$$

$$p(z) = \frac{1}{(2\pi)^2} \int_{BZ_{\parallel}} d^2\mathbf{k}_{\parallel} \sum_v |\langle z | E_v \mathbf{k}_{\parallel} \rangle|^2 (1 - f(F_h - E_v))$$

The influence of free carrier charge redistribution and macroscopic polarization fields are included by solving the *Poisson equation*:

$$\frac{d}{dz} D(z) = \frac{d}{dz} \left( -\epsilon \frac{d}{dz} V_H + P \right) = e(p - n + N_D^+ - N_A^-)$$

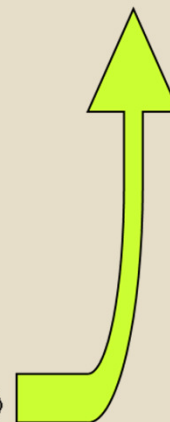
+ **boundary conditions**



$$H = H_C + V_H$$



$$|E_i \mathbf{k}_{\parallel} \rangle$$

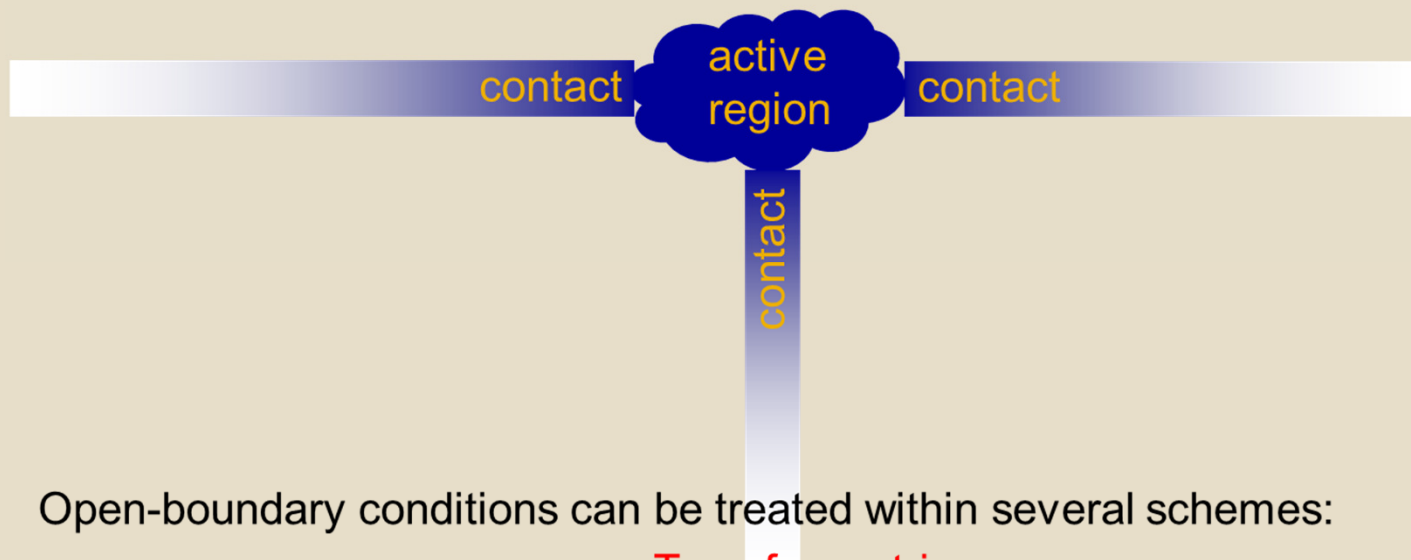


# Boundary Conditions for Transport



The transport problem is:

active region where symmetry is lost  
+  
contact regions (semi-infinite bulk)



Open-boundary conditions can be treated within several schemes:

- Transfer matrix
- Green Functions

These schemes are well suited for localized orbital approach like TB

# Conclusions



- Nanoelectronics has revolutionized in many ways our every day life.
- It has made significant impact in fields like medicine in terms of diagnostics and surgical interventions.
- There are many alternative paths and ways in which future nanoelectronics research might go.
- Atomistic simulations will definitely be of crucial importance and need for understanding future nanoelectronic devices
- Parallel computing will be essential for performing multi-million atomistic simulations.